Comptes Rendus

Géoscience

Sciences de la Planète

Olivier Bellier, Edward Marc Cushing and Michel Sébrier

Thirty years of paleoseismic research in metropolitan France

Seismicity in France / *Sismicité en France*

Thirty years of paleoseismic research in metropolitan France

Olivier Bellier [*, a, b], **Edward Marc Cushing** [c] **and Michel Sébrier** [d]

[a] Aix Marseille Univ, CNRS, IRD, INRAE, Coll France, CEREGE, Aix-en-Provence, France

[b] Aix Marseille Univ, CNRS, ECCOREV, Aix-en-Provence, France

[c] Institut de Radioprotection et de Sureté Nucléaire, Fontenay-aux-Roses, France

[d] Sorbonne Univ., CNRS, ISTEP, Paris, France

E-mails: bellier@cerege.fr (O. Bellier), edward.cushing@irsn.fr (E. M. Cushing),
michel.sebrier@upmc.fr (M. Sébrier)

Abstract. A critical review is conducted of a selection of paleoseismic works published on, or close to, metropolitan France over the last 30 years. The evolution of these works may be subdivided into three periods: dawn of French paleoseismic studies (≈1990–1995), beginning of a multidisciplinary paleoseismologic approach, and paleoseismic studies in the first decades of the 21st century. This review of the most interesting paleoseismic studies at nine trench sites indicates that it is often difficult to associate Quaternary surface deformations with a well-identified fault. However, these studies also provided important results demonstrating that even in regions of low seismicity, seismic ruptures can repeat on the same low slip rate fault, thus providing evidence that historical seismicity is not sufficient to assess seismic hazard in metropolitan France. Finally, recommendations are provided for future paleoseismic investigations in low-seismicity regions.

Keywords. Paleoseismicity, Metropolitan France, Active fault, Quaternary earthquake, Surface rupture, Seismic hazard.

1. Introduction

Paleoseismology was developed by US geologists, at the turn of the 1960s and 1970s to address the lack of historical earthquake records in the western states, with the goal of identifying and characterizing past earthquakes beyond the scope of instrumental seismicity. The overall methodology used to identify paleoseismic events can be summarized as the search for evidence (or clues) preserved in Late Quaternary sedimentary deposits associated with their cumulative effects on the landscape. These paleoearthquakes are determined either directly through the discovery and analysis of their past ruptures at or near the surface, or indirectly, through changes in the past geological and geomorphic environments. This indirect approach, which is not the subject of this review paper, is a specific branch of paleoseismology that attempts to associate recorded effects (lake destabilization, disturbance of sediments—liquefactions, sedimentary veins, landslides, block falls and by extension the disorders to ancient constructions by archaeoseismicity) of earthquakes whose location and source are not necessarily identifiable. To analyze the direct earthquake effects,

---

* Corresponding author.

paleoseismology requires the identification of active faults in order to associate past surface ruptures with their seismogenic characteristics (past earthquake locations, magnitudes, average return periods, etc.). Hence, these paleoearthquake data permit to extend the temporal scales provided by the instrumental and historical seismicity to the prehistoric time period. Thus, paleoseismic studies allow for improved the hazard analyses (e.g., prior to the construction of nuclear facilities). This method was first used in regions characterized by moderate to high level of seismicity (i.e., the central and western United States). In parallel with these first paleoseismic studies, mapping work or compilations were also performed to obtain the most comprehensive view of faults capable of producing significant earthquakes (e.g., $M \geq 6$). A detailed report of the methods and origin of paleoseismology is provided in McCalpin [2009]. Paleoseismic researches also contributed greatly to basic research about fault seismogenic behavior and seismogenesis. These researches have spread worldwide among seismic regions and many studies are now conducted each year (average of ~100/year of published works worldwide since 2003, Figure 1).

The objective of this paper is to provide a critical review of the paleoseismic studies that have been conducted in metropolitan France during the past thirty years. Metropolitan France is characterized by a low level of seismicity, although damaging earthquakes (intensity $\geq$ VIII MSK) have occurred in several locations, one to three times per century, with magnitudes estimated to be approximately in the range M_w 5.0–6.5 [e.g., Manchuel et al., 2018] including the Le Teil earthquake. Faults slip rates associated with this seismicity appear to be very low ($\ll 1$ mm/year, see Section 3). Thus, paleoseismic information should be of primary interest in regions with very low deformation rates to try to better understand the low slip rate faults' behavior. However, is it possible to conduct such paleoseismic studies, with enough confidence in such regions? To address this question, we first present the evolution of the paleoseismic investigations in metropolitan France, which is summarized in three steps (see Section 2). Next, we conduct critical analyses of nine selected trench sites that document the most relevant paleoseismic studies (see Section 3). These critical analyses provide insight into the most interesting results obtained by paleoseismic studies as well as their lim-
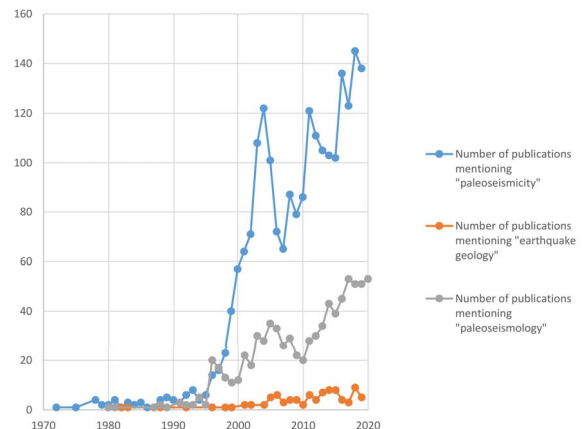

Figure 1. Number of worldwide published papers per year with keywords: (1) Paleoseismicity, (2) Paleoseismology, (3) Earthquake Geology (Scopus database for 1970–2019 period). This to be compared with the 16 peer reviewed publications for Metropolitan France and close surroundings between 1997 and 2021, with a maximum of 4 publications in 2005.

itations or uncertainties so that their conclusions can be reevaluated in the light of current knowledge and experience. In several cases, the most critical point is the identification of the active fault and its relationship to the potential surface rupture(s). All the strengths and weaknesses of the paleoseismic studies presented in metropolitan France are discussed. Finally, the conclusions propose a summary of the main results obtained during the last thirty years and some recommendations for future studies in regions with low seismicity.

2. Evolution of paleoseismic investigations in metropolitan France

2.1. *The beginnings of paleoseismology in metropolitan France (1990–1995)*

In metropolitan France, the development of paleoseismic studies started in the early 1990s. From this beginning until now, three time periods may be distinguished. Following the example of studies carried out in the field of nuclear installation safety on a global scale and following significant earthquakes that had impacted this type of installation
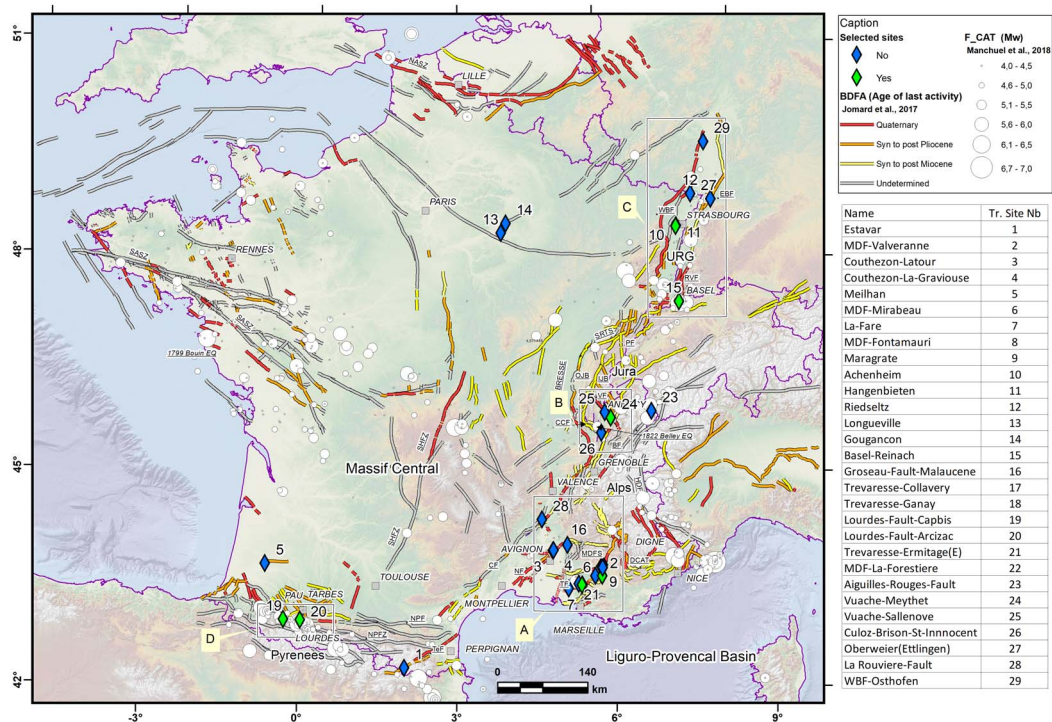
Figure 2. Location of paleoseismological trench sites performed to date in metropolitan France and close surroundings. Main fault systems are drawn from Jomard et al. [2017, and references therein] (cf. BDFA, French potentially active faults database, https://bdfa.irsn.fr). Described region settings are: A, Provence; B, Jura; C, Upper Rhine Graben (URG); D, Central–Western Pyrenees. The trench site (29), though being outside of the area, is included, since it belongs to the URG. Detailed information on trenches are reported in Table A1. Background topography: NASA Shuttle Radar Topography Mission (SRTM) Version 3.0 and General Bathymetric Chart of the Oceans (GEBCO).

[i.e., 1988 Spitak Nuclear power Plant, Armenia—see Griffin et al., 1991]. Studies were carried out to determine whether paleoseismic events had occurred in regions where nuclear installations were already located, using trenches on already identified faults, without implementing a complete approach to identify the more favorable locations using this method. These first studies (see Figure 2 and Table A1) focused on the Nîmes Fault (NF) with a trench at Courthézon, Vaucluse [Carbon et al., 1995, Combes et al., 1993] and on the Middle Durance Fault (MDF) in the Valvéranne valley (see Section 3.1.3) north of Manosque [Sébrier et al., 1997]. Other sporadic paleoseismicity studies were also conducted by IPSN/GEOTER (mainly unpublished reports) in SE France: La Fare Thrust Fault, Mirabeau and Fontamauri on the MDF near a reported Quaternary deformation [Villéger, 1983], Vinon-sur-Verdon (north

of the village) and on the Bersezio Fault in the southern tips of the French–Italian Alps [Ghafiri, 1995]. These trenches were not conclusive given the very poor Quaternary sedimentary settings specific to this region. It should be noted that as part of the ITER preliminary program, a trench showing a fault affecting Pliocene up to early Quaternary deposits was also excavated in 1995, in the south of Vinon-sur-Verdon [see in Thomas et al., 2020].

Parallel to these trench investigations, studies have focused on indirect paleoseismic signatures in lake sediments [e.g., Beck et al., 1996, Chapron et al., 1996, Kremer et al., 2020] and possible disorders on cave speleothems [e.g., Lemeille et al., 1999a], which remains controversial since other causes of speleothem breakages are possible [glacial creeping for example; see review in Gilli, 2005].

Finally, the "French" approach at that time focused on a first list of "evidences of deformation" affecting the Plio-Quaternary [e.g., Grellet et al., 1993, Baize et al., 2002] based on an analysis of the literature (including unpublished reports), geological map booklets, or local to regional studies not necessarily addressing paleoseismic topics (e.g., geomorphological papers, very local observations from geologists, etc.).

2.2. *Emergence of the multidisciplinary paleoseismic approach (1995–2000)*

The study of the Plio-Quaternary deformation evidences showed its limits, as it was not simple or possible, with some exceptions, to link them to potential surface rupture [Baize et al., 2002] and very little indications in terms of paleo-magnitudes, age, and return period of paleoseismic events. While the first trench studies (Courthézon, Valvéranne) seemed promising and confirmed the possibility of active faults that could produce significantly stronger earthquakes than those listed in the French historical seismicity catalog, the approach was only focused on local studies of very few sites located on a fault considered active.

The Annecy earthquake in July 1996, occurred on a well-known fault that was associated with some Quaternary deformation evidences while the earthquake area did not have any record of historical earthquakes. This was the first time in France that a significant earthquake occurred on a well-identified fault whose rupture is reported to have reached the ground surface [Thouvenot et al., 1998]. This event probably contributed to accelerate paleoseismological works in France.

The study in 1996 of the Bree Fault by the Royal Observatory of Belgium [Camelbeeck and Meghraoui, 1998] and the impetus given to a first European scale program of multidisciplinary paleoseismic studies initiated many investigations in Western Europe, including regions bordering metropolitan France (E.U. Paleosis, SAFE, FAUST projects, . . .). Multi-scale approaches using different techniques ranging from morphotectonic analysis of Digital Elevation Models (DEM) at different resolutions, to subsurface geophysics (Ground Penetrating Radar—GPR, ERT, High-resolution seismic reflection/refraction) and the implementation of

various dating methods (^{14}C, ^{10}Be, OSL, . . .) have enabled better identification of the seismic sources and their potential [e.g., Lemeille et al., 1999b, Lacassin et al., 2001, Meghraoui et al., 2001, Ferry et al., 2005, Chardon et al., 2005].

2.3. *Paleoseismic studies in the beginning of the 21st century*

During the first decade of the 21st century, some paleoseismicity studies were carried out in southeastern France, particularly along the Trévaresse Fault [Lacassin et al., 2001, Chardon and Bellier, 2003, Chardon et al., 2005, 2009] and the MDF [Siame et al., 2004, Cushing et al., 2005, 2008]. In the Pyrenees, one can quote the work of Alasset and Meghraoui [2005] and in the Upper Rhine Graben (URG) those of Meghraoui et al. [2001] and Ferry et al. [2005]. Nevertheless, the interest for paleoseismicity using trenching observations in metropolitan France has rapidly declined and there have been only few works between approximately 2005 until 2015 [see Table A1, Baize et al., 2011, De La Taille, 2015]. On the other hand, more integrated studies aimed at completing the parameters useful for the development of seismic hazard assessment have increasingly emerged, combining quantitative geomorphology, morphotectonics, geophysical and structural geology approaches to define seismic potential and slip rates on the basis of displacement of geomorphic features [e.g., Siame et al., 2004, Cushing et al., 2008, Baize et al., 2011, Billant et al., 2015, 2016, Godard et al., 2020]. Dating, which is crucial for determining fault slip rates, can essentially only be carried out by in situ sampling, and trenching, or "pits" (see Section 3).

3. Some case studies of paleoseismic investigation in metropolitan France for 30 years

Selected examples of published paleoseismic studies based on trench observations are presented below. These nine examples correspond to the most relevant paleoseismic studies performed within metropolitan France during the past 30 years. They belong to the following seismotectonic settings: Alpine frontal deformations in Provence (Trévaresse, NF, and MDF—trench sites #2, 3, 9, 21 in Figures 2 and 3) and southern Jura (Vuache Fault—trench site #24 in Figure 2), URG faults (Achenheim–Hangenbieten close

to Strasbourg, Reinach–Basel Fault in the Basel area where the strongest western European earthquake occurred in 1356—trench sites #10 and 15 in Figure 2), and Pyrenean northern seismic zone (Lourdes Fault—trench sites #19, 20 in Figure 2). Most recent works are not included since research is still in progress [Ritz et al., 2020, 2021a,b, Reicherter et al., 2020].

3.1. *Seismotectonic setting of Provence*

Although Provence is characterized by moderate instrumental seismicity, it has experienced a few damaging earthquakes during the last centuries, such as the 1909 Lambesc earthquake or the 1509 and 1708 Manosque earthquakes (SisFrance, M_w ranging between ~5.5–6.1 [Baroux et al., 2001, Manchuel et al., 2018, Stich et al., 2005]. However, Provence active faults are characterized by slow slip rates (≤0.1 mm/yr) [e.g., Siame et al., 2004, Chardon et al., 2005], consequently they have long recurrence intervals and can experience rapid erosion under a Mediterranean climate where morphotectonic signal is rapidly erased.

The active deformation in France and particularly in southern Western Alps and Provence might not be directly associated with the convergence between the African and Eurasia, this convergence being mostly accommodated along the plate boundary south of the Western Mediterranean [Nocquet, 2002]. Consequently, the cause of the Provence deformations is still widely debated and various factors are discussed in the literature [Baroux et al., 2001, Cushing et al., 2008, Le Pichon et al., 2010, Bellier, 2014, Mazzotti et al., 2020, Nocquet, 2012, Walpersdorf et al., 2015, Mathey et al., 2021, Larroque et al., 2021].

Provence is located at the limit of three major morpho-structural domains: the Alps to the NE, where the crust is thickened, the Massif Central to the NW, where crust and lithospheric mantle are thinned, and the western Mediterranean to the south, where oceanic crust is present in the Liguro-Provençal basin (Figure 2) [see Section 4.2 in Larroque et al., 2021]. These different areas are the result of a tectonic history that is characterized by alternations of compressional and extensional deformations in time and space [e.g., Bestani et al., 2016]. The Pyrenean episode created east-west-trending ramp anticlines distributed from the Mediterranean coast

up to north of the Ventoux–Lure mountain, these were subsequently reactivated as normal faults during the Oligocene–Early Miocene regional extension, associated with the opening of the Liguro-Provençal oceanic basin [Hippolyte et al., 2012, Roure et al., 1992, Larroque et al., 2021]. During the Neogene shortening, earlier Pyrenean structures were reactivated resulting in north- and south-verging thrust faults [Chardon and Bellier, 2003, Combes, 1984, Villéger and Andrieux, 1987]. Crustal-scale NE-trending NF and NNE-trending Middle Durance Fault system (MDFS) were simultaneously reactivated as left-lateral strike-slip faults. Then, from the Mid-Miocene onwards Alpine deformation (probably resulting from the collision between the Adriatic block and the European margin) started propagating southward making Provence region the foreland of the Alps [Baroux et al., 2001, Champion et al., 2000, Molliex et al., 2011].

Analysis of geological marker offsets on balanced cross sections [Bestani et al., 2015, Champion et al., 2000], [Chardon and Bellier, 2003] confirm that tectonic deformation is slow (≪1 mm/yr) [e.g., Siame et al., 2004, Chardon et al., 2005, Chardon and Bellier, 2003, Cushing et al., 2008]. In addition, assessment of fault activity based on morphological evidences is subdued because denudation rates are comparable to or faster than fault slip rates [about 30–60 mm/ka: Godard et al., 2016, Molliex et al., 2011, Siame et al., 2004, Thomas et al., 2020, 2018]. This implies that tectonic geomorphic markers tend to be erased, hence, no single stand-alone method can be used to accurately evaluate seismic deformation.

Furthermore, comparison of earthquake focal mechanisms, fault kinematics and Quaternary deformation analysis suggest a change in tectonic regime during the Quaternary. Clauzon et al. [2011] displayed that the main tectonic episode affecting Luberon mountain range, occurred around 5.9 Ma. This means that the deformation of the Luberon ends in Messinian and that the deformation front then propagated southward up to the Trévaresse and possibly to the Aix-Eguilles and La Fare ranges [Figure 3; Terrier et al., 2008].

The length of the fault segments deduced from the structural segmentation allow to estimate a M_w ~ 6.5–6.7 potential maximum magnitudes of earthquakes on Provence faults. However, the contribution of aseismic deformation is unknown. Given the
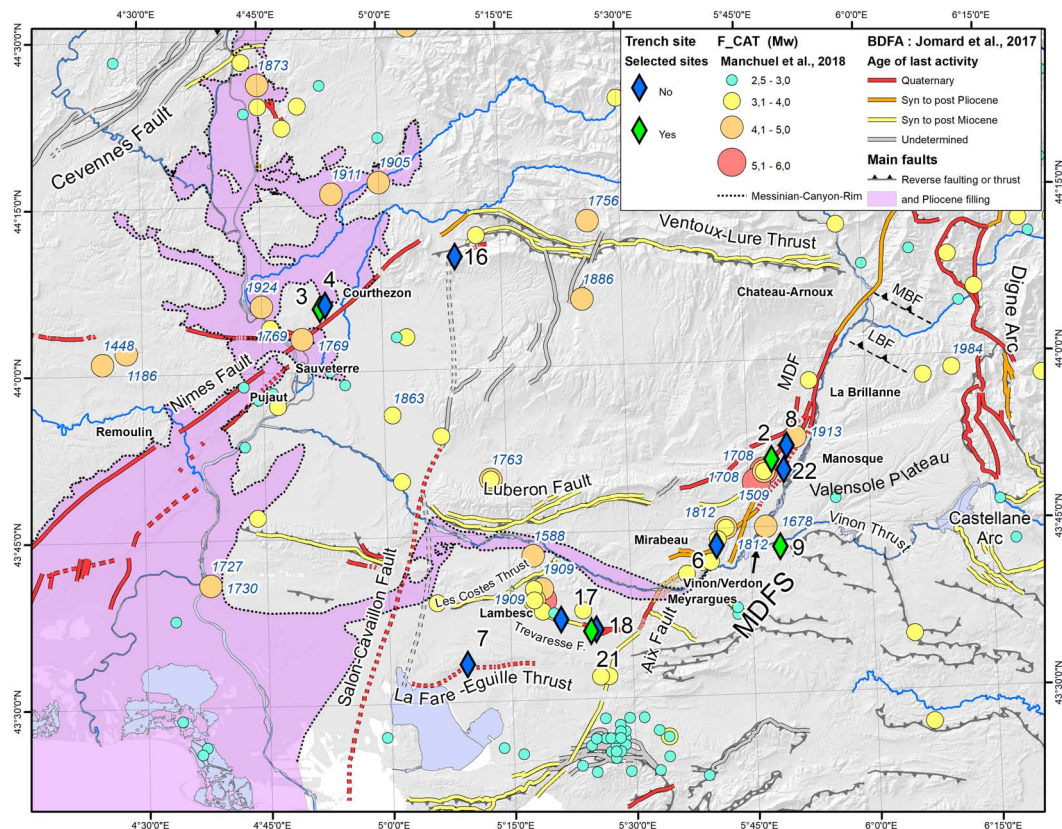
Figure 3. Location of trench sites performed in the Provence area. Faults are reported from BDFA, https://bdfa.irsn.fr. Historical seismicity from the F_CAT catalog [Manchuel et al., 2018]. The Messinian canyon (purple) is drawn with its rims. Background DEM at 25 m resolution is from Institut Géographique National (https://geoservices.ign.fr/documentation/diffusion/telechargement-donnees-libres.html#bd-alti-25-m).

time window of historical seismicity (about 500–1000 years in this region) with maximum estimated magnitude on the order of $M_w \sim 6.0$ and the estimated potential of the slow active faults of Provence ($M_w \sim 6.5$), historical earthquakes probably do not account alone for the seismic hazard. Even though outcropping faults are relatively well known, there are some indications that deep, blind faults with possible higher seismic potential exist such as the Lambrussier, or Mirabeau reverse faults [Figure 3, Godard et al., 2020, Hippolyte and Dumont, 2000].

Clusters of historical earthquakes [e.g. 1769, 1873, 1924, 1905, 1911 earthquakes in Figure 3, see e.g. Larroque et al., 2021] and paleoseismic activity are reported from the main Western Provence boundary faults [Carbon et al., 1993, Dutour et al., 2002, Sébrier et al., 1997]. In addition, combined macro-

seismic, geological and seismological data indicate that the 1909 Lambesc earthquake (Figure 3) took place on the south-verging Trévaresse thrust, a ramp located beneath the Trevaresse ridge anticline, within Western Provence [Lacassin et al., 2001, Baroux et al., 2003, Chardon and Bellier, 2003, Chardon et al., 2005, 2009].

3.1.1. *The Trévaresse Fault*

Geological, geomorphic and topographic field investigations, 50-cm-resolution aerial ortho-photograph interpretation, and DEM analysis conducted in the epicentral zone of the 1909 Lambesc earthquake ($M \sim 6.0$) allowed mapping of the Quaternary deposits and fault traces of the piedmont of the Trévaresse ridge anticline (BDFA, 2020; fault near location 17, 18, 21 on Figure 3), and to constrain

the geometry and kinematics of the Trévaresse fault responsible for the 1909 earthquake [Chardon et al., 2005]. This reverse fault consists of two E- to WNW-striking segments (WTF and ETF on Figure 4A) and is associated with an upper Neogene south-verging ramp anticline. The eastern segment (ETF on Figure 4A) put in contact the Oligocene overthrusting Miocene and is connected at depth and on their eastern tips to two reverse faults (Ermitage Fault: EF and Fauchonne Fault: FF, Figure 4A) mapped ~500- and ~700 m south of this major fault. The emergence of the fault in streams that cut the piedmont of the ridges is marked by a N100° E-trending ramp anticline [Chardon et al., 2005, Chardon and Bellier, 2003].

The recent deformation has propagated in the southern piedmont of the anticline forming a frontal ramp associated with anticlines that are located 500 m and 700 m south of the main topographic escarpment (Figures 4A, 4B, 4C). The microtopography of the abandonment surfaces of the Quaternary fans located at the piedmont of the anticline as well as the longitudinal topographic profiles of the talwegs (dry beds) provide evidence for the relationships between the morphogenesis of the piedmont and the reverse faulting of the Trévaresse. These investigations allowed to target the location and then the excavation of a paleoseismological trench in the Rissian fan of upper Middle to Late Pleistocene age (100–300 ka, deduced by regional correlation) [Nguyen et al., 2007, Chardon et al., 2005, 2009].

Paleoseismological studies. Across the Trévaresse Fault, a 55 m long trench (Figures 4B, 4C, 4D) was excavated across the piedmont fault scarp affecting fan surface, where fan deposits rest on S-dipping Tortonian beds making the southern limb of an anticline. Connected fault splays cuts across the overturned contact between Tortonian shales and fan deposits suggesting for an in-sequence propagation of the thrust fault into successive colluvial wedges.

The latest event is evidenced by the propagation of the uppermost fault splay (Eh5 on Figure 4) characterized by an emerging ramp cutting through the top calcrete horizon with a 20 cm offset of the base of the modern soil horizon, suggesting this could be the surface rupture of the 1909 earthquake. The southern boundary of the hanging wall fan remnant coincides with a south-dipping, north-verging flexural-slip fault (Figure 4B). Surface rupture is not established here, but fan deposits show internal deformation marked by a spaced cleavage that is linked to slip of a bed-parallel fault splay that brought Miocene marls above fan deposits (a on Figure 4B). At the northern tip of the trench, fan deposits record a paleo-rupture event along a flexural-slip fault showing a coseismic slip of 27 cm (c on Figure 4B). This scarp and derived colluviums were buried below a younger aggrading fan sequence (fan deposits in Figure 4B).

The coseismic offsets measured on fault splays range from 19 to 27 cm, corresponds to $M_{\rm w}$ 6.3 ± 02 earthquakes considering Wells and Coppersmith [1994] empirical relationships. Average earthquake fault displacements observed in the trench and segment lengths yield the same order of moment magnitude estimates [Chardon et al., 2009, 2005, Chardon and Bellier, 2003].

The successive colluvial wedges dragged against the Miocene beds have similar thicknesses, suggesting that 7–10 earthquakes of equivalent magnitudes have reactivated the fault. A slip rate of the fault ranging from 0.05 to 0.3 mm/y has been estimated considering the Rissian fan's age that ranged from about 100 to 300 ka and the fan's vertical offset, imaged by electric resistivity tomography [Chardon et al., 2005], which is consistent with displacement rates derived from late Miocene layers [Chardon and Bellier, 2003]. Considering a characteristic coseismic slip of about 20–25 cm and these slip rate estimates, recurrence intervals between 700 and 5000 yr have been proposed.

The trench excavation revealed the emergence at the surface of a fault that generated several paleoearthquakes associated with surface ruptures during and after the fan emplacement. The coseismic fault, affects the base of the present soil and could correspond to the 1909 earthquake rupture. Given the observed incremental displacements, the estimated magnitude of these paleoearthquakes could be similar to that of the 1909 earthquake. The Trévaresse trench indicates that earthquakes repeated on the same fault. This is probably the best evidence in metropolitan France that reverse faulting earthquakes have occurred repeatedly on the same fault.

3.1.2. *The Nîmes Fault system*

The NF trace is generally difficult to discriminate in the landscape, consequently the NF mapping and
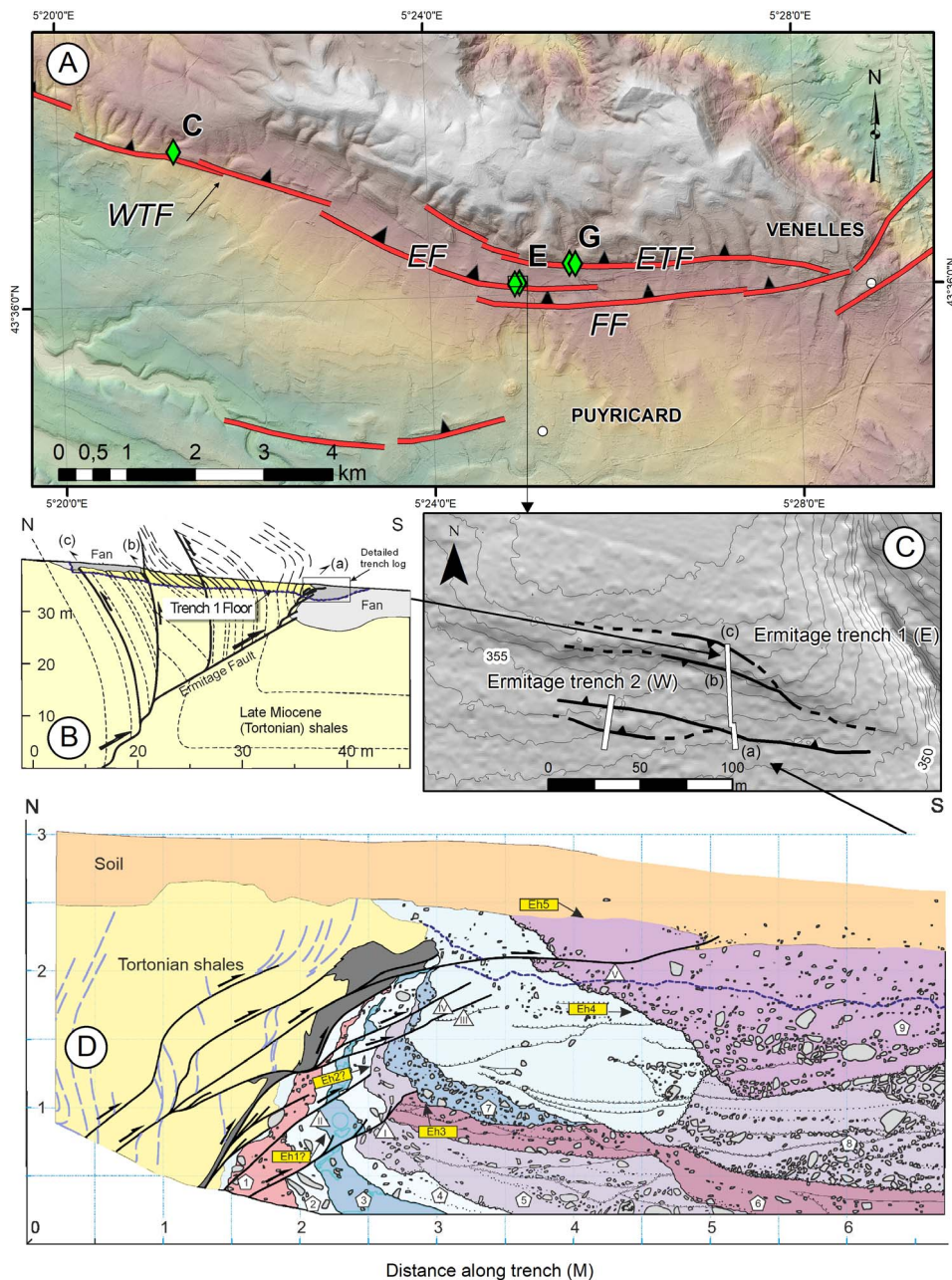
Figure 4. Figures illustrating the Trévaresse paleoseismicity study. (A) Location of faults and of paleoseismicity trenches on the southern limb of the Trévaresse anticline. Trenches names (green diamonds): C = Collavery, E = Ermitage, G = Ganay. Fault Names: WTF: West Trévaresse Fault, ETF: East Trévaresse Fault, EF: Ermitage Fault, FF: La Fauchonne Fault. Location information and fault locations are from Chardon et al. [2005, 2009] and Nguyen et al. [2007]. (B) Middle scale cross section along the Ermitage T1 trench modified from Chardon et al. [2005]. (a), (b), (c) are the location of trenches log presented in Chardon et al. [2005] and also located on the map presented on the Figure 4C. (C) Detailed map on the Emitage–Ganay area (DEM 1 m resolution, https://geoservices.ign.fr/documentation/diffusion/telechargement-donnees-libres.html#rge-alti-1-m, IGN) showing 1 m spaced level curves. Both trenches T1 and T2 are located. The Ermitage Fault and associated splays are mapped. (D) Southern trench T1 log ((a) on Figures 4B and 4C) modified from Chardon et al. [2005] showing the southernmost fault offsetting the soil of which the base displays a 20 cm reverse offset probably by the 1909 earthquake faulting [Chardon et al., 2005]. Units (numbered pentagons) 1–7 are interpreted by Chardon et al. [2005, 2009] as colluvial wedges that could be associated with coseismic displacements. Roman numbered triangles identify five fault splays. Chardon et al. [2005] identified an earlier faulting acting on splays I and II and more recent events mobilizing splays III, IV and V. Only splay I and V provide evidence for coseismic surface ruptures. We identified five possible event horizons numbered 1 to 5 on the figure.
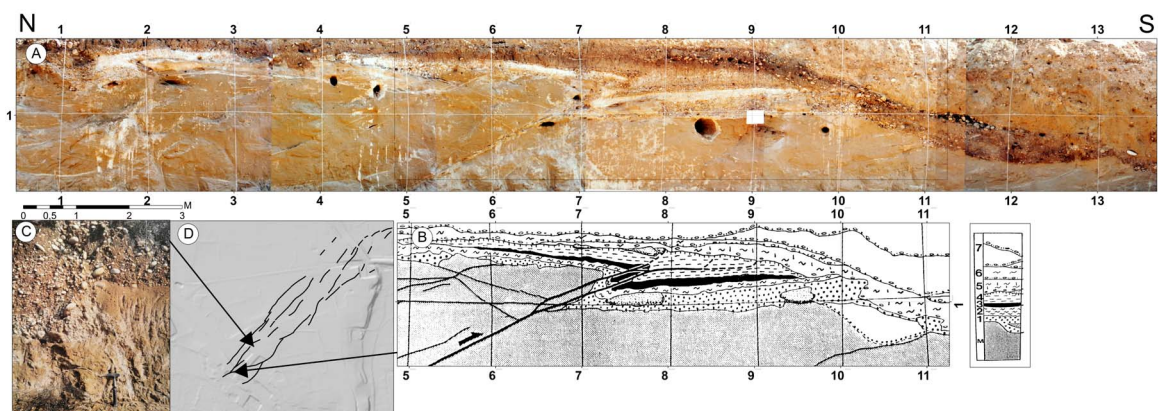
Figure 5. (A) Photomosaic reconstructed from original pictures taken during logging in the Courthézon-Latour Trench (data GEOTER/IRSN, 1992). The log is from Combes et al. [1993]. The Log (B) shows the lithologic succession: M = Langhian–Serravallian sands; 1, 2 fluvial terrace (coarse to fine); 3, 4 fluvial terrace (fine, with white clay), flooding facies overlain by coarse fluvial terrace level; 5: Coarse flooding facies weathered by a fersialitic brown (historic) paleosoil with low decarbonatation and containing gastropods; 6: truncating body (colluvium reworking Miocene sands and the previous paleosoil, containing roman (R) tiles); 7: modern backfill. Levels M to 5 are clearly affected by faulting, the truncating formation is sealing the deformation. The fluvial terrace has not been dated and is attributed to the "Rissian" period (Middle Pleistocene). (C) An older terrace (Upper Lower Pleistocene) is reversely faulted a few hundreds of meters east next to the "Cellier des Prince" wine cellar. (D) Location of the Courthézon-Latour Trench and the "Cellier des Princes" outcrop.

segmentation is difficult to establish because the associated morphological signal is tenuous [Capella et al., 2014, Peulvast et al., 1999, Schlupp et al., 2001]. The NF (Figure 3) was reactivated in the Upper Miocene with a left-lateral strike-slip component [e.g., Champion et al., 2000, Schlupp et al., 2001]. The NF appears more clearly 50 km north of Remoulin and it has been considered to be active in the Quaternary north of Sauveterre (Figure 3) by Grellet et al. [1993]. Several features of Plio-Quaternary deformation have been observed near the fault trace, notably close to Courthézon (Figures 3, 5) where one example of paleoseismological deformation exists [movement on a reverse fault affecting a Middle Pleistocene terrace; Combes et al., 1993, Carbon et al., 1993].

An attempt to quantify the Plio-Quaternary strike-slip component of the NF was carried out by Schlupp et al. [2001], using the infilled Messinian Rhone river canyon (mapped on Figure 3) as deformed markers. The results of this study have been widely discussed [Schlupp et al., 2001, 2002, Mattauer, 2002, Séranne, 2002]. Later works confirmed post-Pliocene reverse component [Clauzon et al., 2004] and transpressional faulting in the Pujaut Basin [Capella et al., 2014].

The Cellier des Princes outcrop [Pascual, 1979, 1978], as well as the reverse faulting component revealed by the Courthézon-Latour trench [Figure 5; Combes et al., 1993, Carbon et al., 1993] agree with the occurrence of a deformation corridor aligned along-strike the NF. It seems that a "post-Rissian" (e.g., about 250,000 to 130,000 yr BP) reactivation of the NF zone is responsible for these associated deformations. Moreover, this Rhône terrace, downstream Courthézon, on the site of Les Saumades, is eroded by the Ouvèze river, implying that the river had reintegrated its western course. The concomitance of the processes suggests that tectonic deformation is at the origin of the recent Ouvèze incision.

Paleoseismological studies at the Cellier des Princes. At the Cellier des Princes, Pascual [1978] described a metric outcrop (presently walled outcrop), where he observed a NE-trending 70° SE-dipping reverse fault affecting Langhian–Serravallian sands ([3, 4] in Figure 5C), location ([3] in Figure 3), as well as a probably Rissian terrace. The apparent vertical thrust offset from the base of the terrace is about 50 cm, the southern fault block moving northward.

Although geophysical investigations (GPR profiles) have been carried out in the vicinity, the section does not permit identification of any clear feature that could be associated with the Cellier des Princes Fault [Baroux, 2000].

Paleoseismological studies at Courthézon-Latour. At the Courthézon-Latour site (location Figure 3 [9]), two 15 m long trenches allowed Carbon et al. [1993] and Combes et al. [1993] to describe several reverse faults. The main trench ([A, B] in Figure 5) provided evidence for a N50° E-trending, 30° N-dipping major fault affecting Miocene sandstones and a terrace attributed to Mindelian (lower Middle Pleistocene) or Rissian (Middle Pleistocene). This fault is sealed by deposits containing Gallo-Roman ceramics of about 2000 years BP. The geometric restoration of the observed shifts led Carbon et al. [1993] to propose two paleoseismic events for an apparent 60 cm cumulative reverse offset. Considering some hypothesis on stress state Carbon et al. [1993] argue for a dominant strike-slip fault kinematics and thus estimate a coseismic slip ranging between 1.7–2 m. They deduced from the scaling law a magnitude of 7 related to this paleo-event. This constitutes one of the less controversial examples of a rupture possibly associated with a paleoseismic event on the metropolitan territory. Despite the absence of a conclusive geophysical study along the NF system, the deformation observed should correspond to one or more earthquake ruptures.

3.1.3. *Middle Durance Fault system (MDFS) and surroundings*

The ~90 km long NNE-trending MDFS (Figure 3) is one of the major fault systems in southern France. It is suggested that the MDFS acts as a southward transfer zone of the external Alpine front in Western Provence from the Digne thrust sheet to the south-verging Trévaresse or Eguilles–La Fare thrust systems [Cushing et al., 2008, Terrier et al., 2008]. The MDFS (Figure 3) divides Provence into two structural domains: the western area consists of a thick Mesozoic to Oligocene sedimentary cover (<12 km) whereas the eastern area presents a thinner sedimentary cover (<2 km) [e.g., Bestani et al., 2015, Cushing et al., 2008, Le Pichon et al., 2010, Molliex et al., 2011]. The MDFS is formed from north to south by two major faults: the NNE-trending MDF and the

N-trending Aix-en-Provence Fault (AF) (Figure 3), these two faults are linked by a complex fault bend zone nearby the eastern tip of the Lower Durance valley, north of Meyrargues.

The MDFS can be divided into four main zones [Cushing et al., 2008] (Figure 3): (1) the northern one, trending N20° E, from Chateau-Arnoux to La Brillanne; (2) the central one trending N30° E between La Brillanne and Mirabeau; (3) the southern one, trending N40° E from the Mirabeau-Beaumont to Meyrargues; and (4) the AF, from Meyrargues and the area to the Eguilles–La Fare thrust. The central part of the MDF exhibits some 6 km of Lias then Oligo-Miocene cumulated normal displacement of the basement top [Roure and Colletta, 1996, Cushing et al., 2008, Le Pichon et al., 2010, Guyonnet-Benaize et al., 2015, Bestani et al., 2016, Larroque et al., 2021, and references therein]. However, the Neogene to Present reverse oblique slip has produced an about 1.5 km vertical displacement which postdates the Miocene [Bestani et al., 2016, Roure et al., 1992, Larroque et al., 2021, and references therein].

The recent and present activity of the MDFS is evidenced by its seismicity at different time scales: (i) The MDF is currently the locus of instrumental seismicity [Cushing et al., 2008]. (ii) Four damaging earthquakes (1509, 1708, 1812, and 1913 with MSK Intensity ≥ VII; Figure 3) occurred in the past five centuries (http://www.sisfrance.irsn.fr). (iii) A paleoseismological study [Sébrier et al., 1997] reported a ~1 m coseismic dislocation (see below). Quaternary deformations have been reported all along the MDF [Villéger, 1983, Terrier, 1991, Siame et al., 2004].

Cushing et al. [2008] proposed a 3D structural segmentation of the MDFS, constituted by 10 segments with lengths ranging from 8 to 18 km. This structural architecture was confirmed by a seismic reflection profile reinterpretation [Guyonnet-Benaize et al., 2015]. Thanks to ten years of seismometer measurements in the vicinity of the MDF [Cushing et al., 2008], focal mechanisms have been computed for events with magnitudes ranging from 1.2 to 2.2. They displayed a dominant left-lateral strike-slip faulting associated with reverse component that results from a NNW-trending compression. A study combining cosmogenic dating and geomorphologic feature analysis yielded a MDF slip rate of about 0.07 mm/yr estimated over the last 70 kyr [Siame et al., 2004]. This low value is on the same order as proposed for

other active faults in Provence, over variable time spans [Schlupp et al., 2001, Chardon and Bellier, 2003, Chardon et al., 2005]. Four trenches were excavated all along the MDF (Figure 3, Table A1), but only the Valvéranne one provides evidence for a possible coseismic displacement.

Paleoseismological studies at Valvéranne. Upper Pleistocene torrential deposits were observed on a roadcut located along the Valvéranne talweg north of Manosque (location [2] in Figure 3), above the westernmost fault segment of the MDF (Figure 6). The deformation represented in the Valvéranne trench is a knee fold affecting 26,800 ± 610 yr BP alluvium and fossilized by a 9123 ± 190 yr BP colluvium level (Event horizon—Eh on Figure 7) [e.g., Sébrier et al., 1997]. The SE-dipping, N35° E-striking fold axis plane (dashed line, on Figure 7) is parallel to the major MDF. Near the axial plane some pebbles are straightened and sheared. The eastward dip of the axial plane changes from 55° to 25°, from the base to the top, respectively. This knee fold, results from a W-verging steep reverse shear fault, i.e., opposite to the local slope dip, hence it cannot result from a local gravity instability. It was interpreted as an evidence of tectonic deformation within the Quaternary [Ghafiri, 1995, Sébrier et al., 1997]. The substratum of the torrential deposits is cropping out along the Valvéranne stream and corresponds to steeply E-dipping Middle to Upper Miocene sandy Molasse, hence the shear corresponding to the knee fold is approximately parallel to the Miocene bedding, suggesting it should root on a steep, W-verging reverse fault approximately parallel to the local Miocene beds. The logging of the Valvéranne roadcut allowed to estimate a shear dip slip of ~1 m. As no evidence for progressive folding was observed within the knee fold, it was considered that the fold was formed during one single ~1 m displacement on the shear plane that may correspond to a near-surface earthquake rupture (Figure 7). As this knee fold was partly eroded and subsequently covered by colluvium, the limit between the torrential deposits and the colluvium was interpreted as the event horizon of a paleoearthquake. According to ^{14}C ages within the torrential deposits and the colluvium, respectively, this paleoearthquake should have occurred between 26,800 ± 610 BP and 9123 ± 190 BP [Ghafiri, 1995, Sébrier et al., 1997, Baize et al., 2002]. Finally, ac-

counting for the ~1 m displacement, the magnitude of this paleoearthquake was estimated as M_w ~ 6.5–6.9 [Sébrier et al., 1997]. The dataset on the MDFS has significantly increased since the Valvéranne paleoseismic results have been published, providing opportunity to revisit these results. Thanks to the analysis of seismic reflection profiles, the geometry of the MDFS is now well-constrained (Figure 6A) and the Valvéranne Fault, localized 3 km W [segment 4 Manosque-Villeneuve East, see Cushing et al., 2008] of the MDF [Guyonnet-Benaize et al., 2015] (Figure 6C). Moreover, the Valvéranne site is associated with a steeply E-dipping fault while the MDF is a W-dipping fault, hence the Valvéranne Fault should be considered as a secondary structure of the MDF. It is locally parallel to the Miocene bedding so that the Valvéranne deformation could correspond to bedding slip, which would accommodate the folding of the Miocene series associated with the MDF slip (Figure 6D). The same type of secondary bedding slip fault associated with a main coseismic rupture is also observed in similar compressive contexts as for example in Tibet and Argentina [Tapponnier et al., 1990, Siame et al., 2015].

The geological cross section of the Valvéranne creek shows a sharp transition between E-dipping Miocene and reversed W-dipping Oligocene series, probably due to a major reverse fault (Figures 6C, 6D). The same geometry is also observed in a trench excavated in 1995 [Grellet et al., 1995, Baize et al., 2002] in the parallel Fontamauri talweg, 4.5 km north from Valvéranne (Figures 6B; 8). Thus, Valvéranne Quaternary deformation would then lie between the two main faults, and close to the western one, identified on the seismic section [Cushing et al., 2008, appendix] (Figure 6C).

In conclusion, the Quaternary tectonic deformation appears well identified at Valvéranne and the paleoearthquake age range remains correct. Such secondary bedding slip is usually observed for $M_w > 6$ events [see Rockwell et al., 2014] for the use of secondary faulting.

The seismogenic potential of the MDF was estimated from source sizes and estimated slip rates to range between M_w 6.0 and M_w 6.5 with a return period of a few thousand years [Cushing et al., 2008], that remains consistent with the potential magnitude estimates from bedding slip behavior.
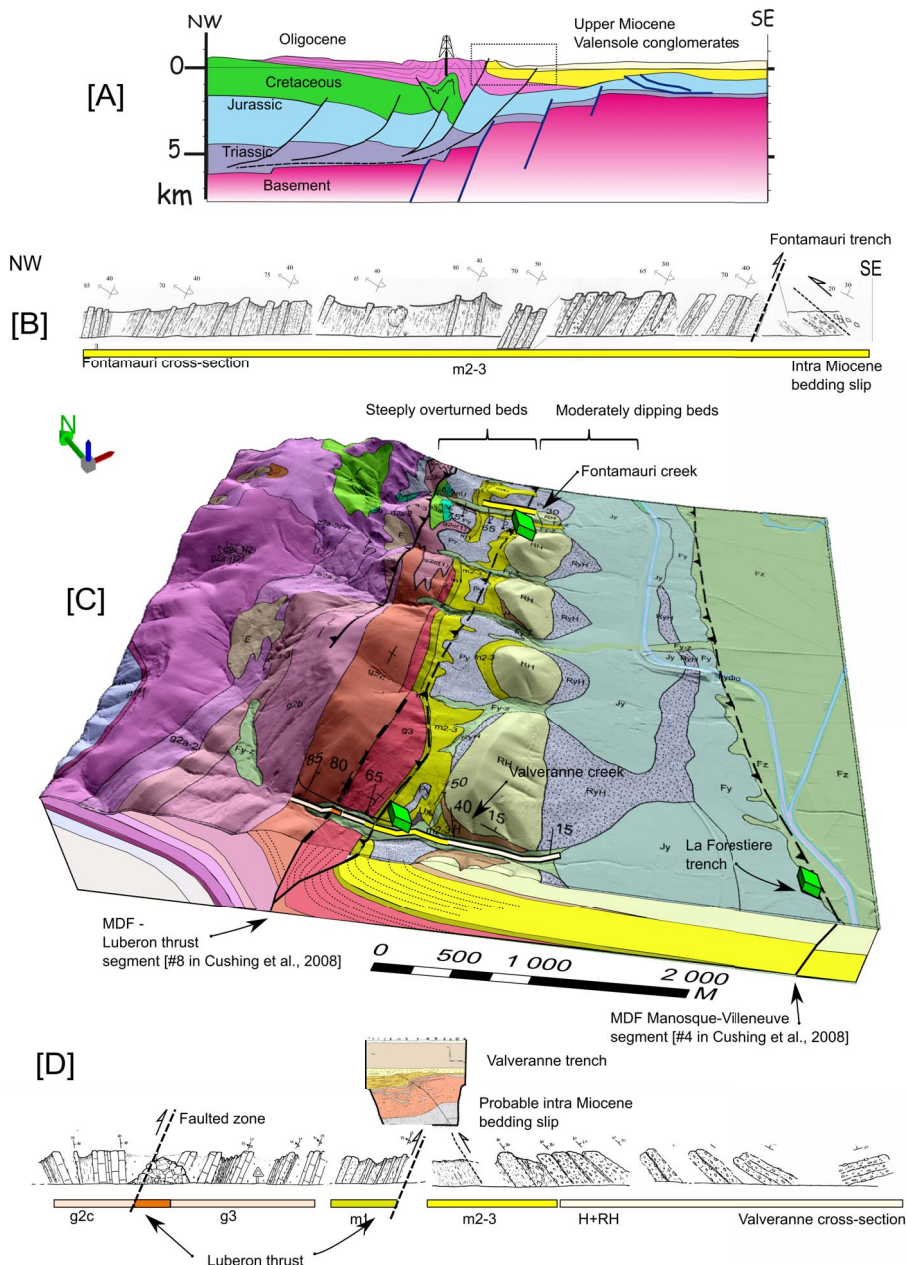
Figure 6. (A) General cross section of the Manosque anticline [adapted from Cushing et al., 2008]. (B) Cross section along the Fontamauri creek showing the overturned beds passing abruptly to conformal geometry at the location of the major fault (Luberon thrust). (C) 3D block showing relationship between the Valvéranne and the Fontamauri trenches/cross sections: both show the same structural setting with a huge reverse fault (Manosque anticline fault) with overturned Oligocene beds at Valvéranne creek and a thick striated gouge zone at Fontamauri. Three green diamonds display locations of trench sites (Valvéranne, La Forestière and Fontamauri). (D) Cross sections along Valvéranne creek shows structure of Oligo-Miocene beds (colored strips for geological stages, g for Oligocene, m for Miocene, H+RH for Miocene Valensole conglomerates). Bedding slip affecting the Miocene series is observed at both sites, in the footwall, of the Fontamauri trench and inferred at the Valvéranne trench. DEM 5 m, https://geoservices.ign.fr/documentation/diffusion/telechargement-donnees-libres.html#rge-alti-5-m, IGN).

Figure 7. (A) Trench log modified from Sébrier et al. [1997] and Baize et al. [2002]. (B) Picture of the Valvéranne trench logging in December 1992 (credit: Ghafiri A.). The picture is presented at about the same scale as the trench log. The bottom of the trench is hidden by the edge of the road in the fo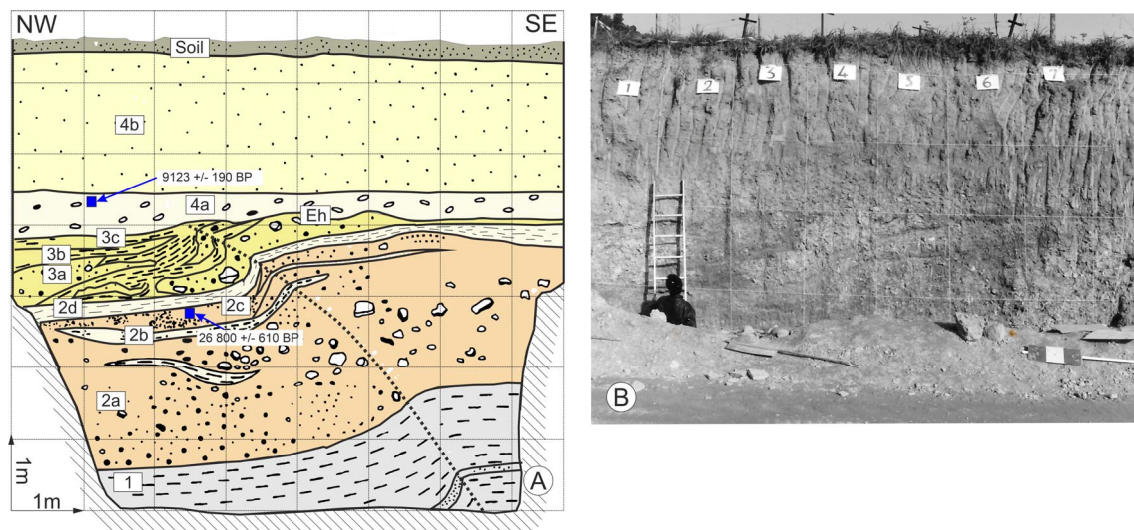reground. Description of the trench series: from bottom to top with (1 to 3) fluvial and torrential deposits overlain by colluvium (4): 1: greenish clay horizon; 2: heterometric coarse level grouping horizons 2a and 2c, in which sandy lenses (2b) are interbedded; 2d: silty-clay level with peat layers, passing laterally to a heterometric coarse horizon; 3a: coarse horizon overlain by two clayey levels (3b and 3c); 4a: gravelly formation passing to silty (4b) one. Radiocarbon dating: • ^{14}C dating from wood fragments sampled in the lower fluvial formation (2c): 26,800 ± 610 yr BP; • ^{14}C dating from carbonate concretions taken in the top part of colluvium (4a): 912 ± 190 yr BP. Upper colluvium age is attributed to Neolithic, as attested by the archaeological markers found (burnt stones and sherds).

Paleoseismic studies at Maragrate. Vinon-sur-Verdon is 8 km to the east of the MDFS, at the toe of the Vinon thrust, an E-trending south-dipping reverse fault [e.g., Tempier, 1987] sealed by Miocene units. South of Vinon thrust, a fault contact between Miocene clays and Pliocene–Pleistocene conglomerates has been observed on a roadside outcrop [Grellet and Combes, 1995 in Thomas et al., 2020]. The conglomerates correspond to the continental Valensole formation which is interpreted as the Durance–Verdon southward prograding alluvial fan system [Clauzon et al., 1989]. Chronological data yield ages ranging between Late Miocene (Serravallian to Tortonian) at its base to early Pleistocene at the top [Clauzon et al., 1989]. At Maragrate (location Figure 3 [9]), this conglomerate unit, more likely Pliocene to Early Pleistocene is deformed along the N120° E-trending Maragrate Fault, as testified by oriented and striated pebbles [Tassy, 2007], consistent with a dextral Plio-Quaternary Maragrate Fault kinematics. Even though instrumental and historical seismicity are documented west of Maragrate along the MDFS, no seismic event has been recorded in the area. Two kilometers to the east of Vinon-sur-Verdon, a 1.5 km long N180°-trending fault segment connects the north Vinon thrust segment (N090°) to the south Vinon thrust segment (N120°), the WNW-trending Maragrate Fault being connected to the south Vinon thrust. The north Vinon thrust does not display Quaternary tectonic activity as Miocene and Pliocene units are lying unconformably on top of folded Cretaceous and Jurassic units, sealing the fault plane. Thomas et al. [2020] proposed that the Maragrate Fault is a sub-vertical fault affecting the sedimentary sequences up to the Pliocene. Thomas et al. [2020] proposed a depth anchoring of this fault connected to the north Vinon thrust approximately 500 meters below the surface, suggesting strain partitioning between the two faults.
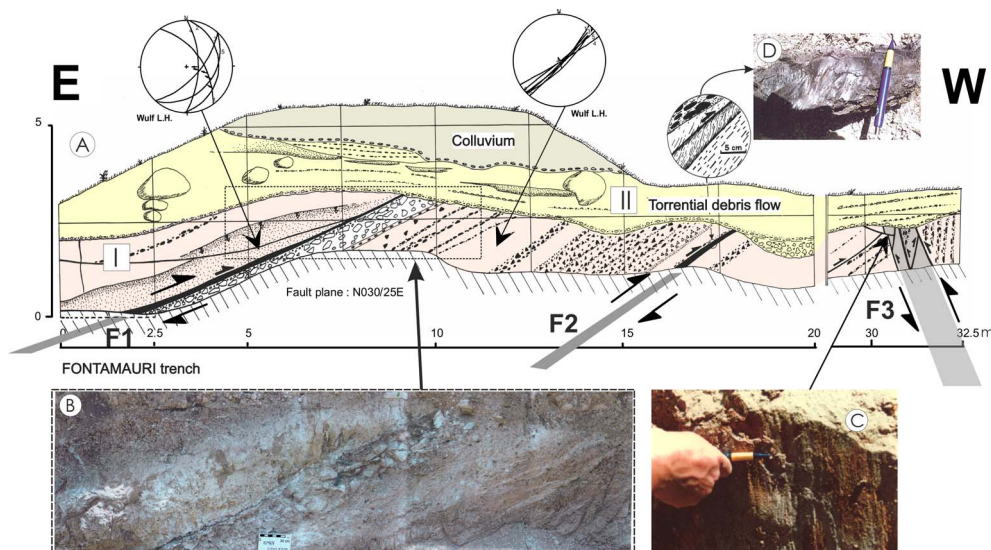
Figure 8. (A) Fontamauri E–W 35 m long trench excavated near Volx village. (B) Photomosaic (detailed zone) of the trench log (displayed within the dashed-line rectangle). The trench displays bedding slip (F1) in lacustrine sediments and conglomerates (I) and a major fault (west) is characterized by dip-slip reverse striae (picture C) in a huge gouge zone separating different dipping domains and probably corresponding to one of the major faults emerging west of Valvéranne trench (F3). Two blackish clay levels mark the presence of two faults parallel to the bedding (F1, F2). Numerous striations (detailed drawing and picture in (D) as well as shear sigmoids indicating a reverse movement were observed (F1: N30°–N40° 25° E; F2: N20° 27° E). Some small secondary reverse faults with high angle dip (70°–80° SE) affect the clay mass located between faults F2 and F3. The Lacustrine series facies differs from regional knowledge description of continental Miocene. The finding of Miocene gastropods would suggest a Miocene or Pliocene age for this series. However, some charcoal sampled contain pine tree pollens which are unknown in the Miocene stage. The torrential debris flow (II—Holocene ?) and the absence of a more developed Quaternary series make it impossible to specify the age of the last movement. In terms of paleoseismicity, the only conclusion possible in the present state of knowledge is the evidence of a post-Miocene and ante-Holocene surface rupture.

Even if the Maragrate contact has been interpreted as testifying for a fault, the question for the relationship between this Quaternary deformation and seismic activities has long been raised. A recent multidisciplinary study has been implemented along this fault [Thomas et al., 2020]. The first challenge in this analysis was uncovering potential deformed Quaternary surfaces and fault scarp morphologies, often found under dense vegetation cover or in urban areas. An extended multi-proxy approach to evaluate this post-Pliocene activity in the context of significant erosion and human activities has been implemented: (1) an airborne LiDAR (Light Detection And Ranging) campaign permitted to produce a 30 cm high-resolution DEM for bypassing the limitation related to the dense vegetation; (2) detailed morpho-logical observations on the DEM, complemented by morphotectonic control field investigation allowed a detailed geomorphological mapping; (3) electrical resistivity surveys were carried out to image the extent of the fault contact at depth. These investigations allowed to decide the location of trenches that revealed a fault contact expressed by a fault gouge zone sealed by numerous recent Quaternary periglacial and high-energy channel units. A sampling was carried out for sedimentology and age constraints (14C and OSL).

At Maragrate, a 300 m long morphological scarp, likely due to differential erosional between the Miocene clay and the Plio-Pleistocene conglomerate fault contact, has been mapped. This scarp is not observed with the LiDAR DEM in the Maragrate valley

because of recent incisions and alluvial deposits. The geophysical survey displayed evidence for the geometry of depositions in the first ten to fifteen meters below the surface and helped to pinpoint a location for the trenches. In trenches, the Maragrate Fault exhibits a shear zone with fault gouge within sediments dated by OSL at ~200 ka [Thomas et al., 2020]. The fault termination is sealed by a fluvio-glacial unit, dated at approximately 18–20 ka with no evidence of recent faulting. There is no evidence that this shear deformation was produced by one or several seismic events, due to the lack of stratigraphic control. Based on segmentation assumptions from the authors (Maragrate fault connected or not to the north Vinon thrust segment, fault rooted at ~2 km maximum, rupture length of about 5 km) the maximum seismic potential associated with this fault would be of the order of $M_w \sim 5$ according to empirical relations of Wells and Coppersmith [1994].

3.2. *Seismotectonic setting of the Jura area*

The 70 km wide Jura Mountains is one of the youngest external fold and thrust belt of the western Alps. Thrusting and folding began by Mid-Miocene while the structure was emplaced at the end of the Miocene forming a ~west-verging arcuate plateau topography [Burkhard, 1990, Laubscher, 1992]. This fold and thrust belt propagated westward on the top of the Oligocene, ~N–S oriented Saone–Bresse graben. To the north, the NE tip of the arcuate structure corresponds to E-striking folds that are overthrust on the rim of the southern URG end, which is connected to the Bresse Graben through the Saone–Rhine transfer fault system. The most characteristic feature of the Jura is its thin-skinned tectonic style marked by faults and folds rooted in the Triassic evaporite detachment. In addition, the Jura is affected by transverse secondary (but extended) structures (such as the Vuache, the Pontarlier, the Cerdon Faults, etc.) that are associated with known historic or recent seismicity (i.e. Annecy $M_w \sim 5.0$, superficial earthquake). In the outer Jura belt, there are no records of paleoseismic data (i.e., rupture affecting Quaternary deposits), while in the Inner Jura belt, few surface deformations are reported even if their tectonic origin is uncertain according to the NEOPAL database [NEOPAL, 2009].

The Jura seismicity is weak and scattered. Several historical events have been recorded with intensity ranging from V to VII. A noticeable event occurred north of Lake Bourget in Belley on 19/2/1822, with estimated magnitude $M_w \approx 5.5 \pm 0.4$ at ~10 km [Manchuel et al., 2018], below the detachment layer located at depth ranging between 2 and 5 km [e.g., Burkhard, 1990]. Consequently, it could be associated to a deep crustal fault anchored below the Cerdon–Culoz Fault in the Jura sedimentary cover [De La Taille, 2015]. More recently the Epagny earthquake (15 July 1996, $4.3 \leq M_w \leq 5.3$) struck the Annecy region (Savoie) causing some building damages.

3.2.1. *The Vuache Fault system*

The Vuache Fault system (Figure 9) connects the southern Jura to the northern subalpine ranges crossing the southern Swiss molassic basin [Thouvenot et al., 1998]. This system accommodates the Neogene shortening difference between the Jura and the Subalpine ranges. It is considered as the SW lateral ramp of the Molasse basin [Philippe, 1995, Thouvenot et al., 1998], constituted by NW-trending left-lateral strike-slip faults that offset the southern Jura NNE-striking folds [Baize et al., 2011, Figure 2], and it has been divided into six segments [Jomard et al., 2017, Baize et al., 2011, De La Taille, 2015; cf. Figure 2]. A segment is revealed by an alignment of 200–300 m long left-lateral talweg inflections [underlined by arrows on Figure 9, Baize et al., 2011] and an approximately 2 km left-lateral shift of a Rhône paleo-drainage [Baize et al., 2011]. Historical earthquakes in 1875, on 17/04/1936, 29/05/1975 (Ml = 4.2, I_0 = V–VI), the Frangy event (Ml = 2.6, 16/11/1983) and the Epagny earthquake (ML = 5.3, 15/07/1996 that occurred NW of Annecy) are associated with the Vuache Fault [Thouvenot et al., 1998; www.sisfrance.irsn.fr]. The Epagny earthquake focal mechanism is consistent with the Vuache left-lateral strike-slip faulting. On the eastern end of the Vuache Fault, under Lake Annecy, a 40 m Holocene sedimentary pile studied by Beck et al. [1996] would indicate evidences for some earthquake-related deformation (ball-and-pillow structure and brittle-like behavior of soft, water-saturated, sediments). A multidisciplinary study conducted by Baize et al. [2011] confirms that the Vuache Fault has a Quaternary activity that is displayed by its footprint in the landscape and Quaternary deposits that seem deformed all along the fault (Figure 9). However, these deformations could be related with glaciotectectonics.
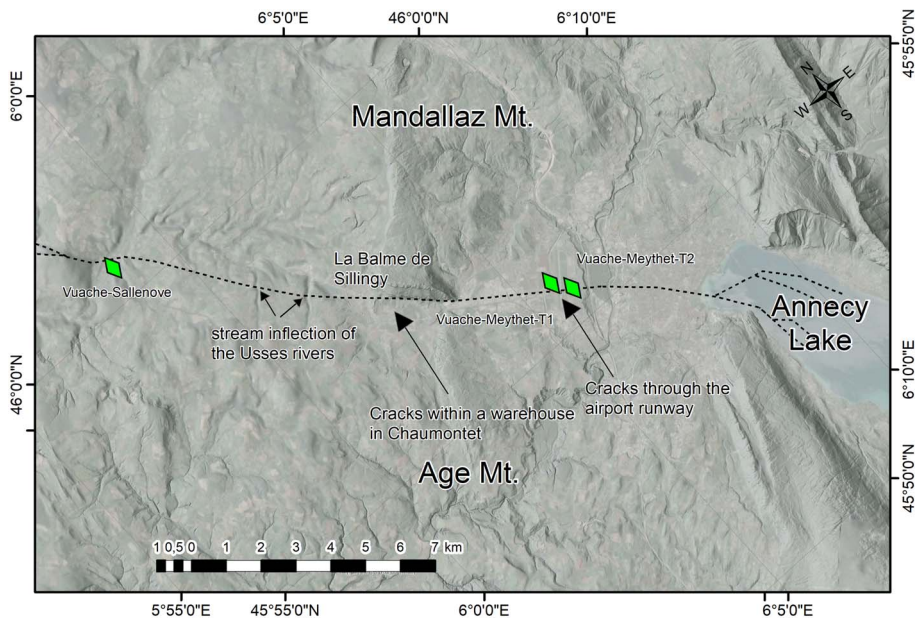
Figure 9. Trench locations indicated with green markers performed in the Annecy area. The dotted black line indicates the surface trace of the Vuache fault [De La Taille, 2015]. The stream inflection of the Usses rivers is indicated by arrows [Baize et al., 2011]. DEM 5 m (https://geoservices.ign.fr/documentation/diffusion/telechargement-donnees-libres.html#rge-alti-5-m, IGN).

Surface faulting and paleoseismological investigations along the Vuache fault. A detailed study was performed in the area of the 1996 aftershocks epicenters [Thouvenot et al., 1998]. It displays evidence for presumed surface rupture and coseismic cracks (N140° E-trending cracks just off and on the runway of the Annecy airport and horizontal displacement and cracks observed within a warehouse south of Mandallaz mount, Figure 9) around the Annecy airport. In order to assess the paleoseismic activity and following subsurface geophysical investigations two trenches were excavated in young fluvial deposits (<10 ka), where thick alluvial gravel (30 m) overlies 150 m of lacustrine clays [Figure 9, Meythet trenches T1 and T2; Baize et al., 2011]. These trenches did not exhibit any clear shear zone and/or crack that could be related to the 1996 or older event. Considering the huge thickness of the coarse fluvio-glacial layer, it is very likely that the paleoruptures have been damped by the unfavorable lithology. In addition, this lack of coseismic surface rupture could result from both the small earthquake magnitude ($M_w = 4.8 \pm 0.5$) and the thickness of the unconsolidated recent sediments that explains why the potential seismic rupture was dampened and unable to propagate to the

surface. This stresses how difficult it is to recognize small deformations in coarse and poorly compacted sediments.

3.3. *Upper Rhine Graben and its southern rim (Jura fold belt)*

The URG is part of the Western European intracontinental rift linking the North Sea to the Western Mediterranean Sea. The URG is nearly 300 km long and 40 km wide, with a moderate mean altitude of the rift floor of some 200 m. The eastern and western graben borders are marked by 70°-dipping NNE-trending normal faults, associated with high altitude shoulders reaching 1000–1500 m in its central part (Vosges and Black Forest). Graben infilling is about 1000–3500 m thick. URG Tertiary layers display dip-slip offsets of some 500 m.

The northern URG is characterized by a Neogene to Quaternary subsidence. In the Heidelberg–Mannheim area along the northern URG eastern edge, 350 m thick Quaternary sediments are affected by normal faulting associated with an extensional tectonic regime [Bartz, 1974]. The corresponding Quaternary subsidence rate estimated is about 0.1–0.2 mm/yr [i.e., Monninger, 1985].

The Jura frontal fault and fold detachment propagated northwards [Philippe, 1995], as far as the Mulhouse horst (Mulhouse–Richeim ramp in Figure 10) according to Nivière and Winter [2000]. Vertical uplift rates on the order of 0.05 mm/yr since the onset of the Quaternary along the Florimont and Réchésy anticlines [Giamboni et al., 2004, FrJuraN 3 and 4 in Figure 10], caused the deviation of the northwards Rhine river course. The southernmost URG, shows Quaternary E-trending thrust ramps indicated by surface anticline growth and by a detachment level rooted at 2–3 km depth [Nivière and Winter, 2000]. The slip rates estimated for these ramps reach 0.16–0.3 mm/year.

The Quaternary activity along the border faults is not documented, except for the NNE-trending western Rhine fault in the northern URG, which has an estimated slip rate of 0.03 mm/yr [Peters et al., 2005] over the Upper Pleistocene, where some gravitational effects might influence the deformation.

In the central URG, morphological markers indicate a reactivation of the west-dipping Rhine River Fault [Nivière et al., 2008; RRF-2 in Figure 10]. The estimated slip rates associated with their Quaternary activity range between 0.04 and 0.1 mm/yr [Bertrand et al., 2005, Nivière et al., 2008]. The roughly N-trending, E-dipping Achenheim–Hangenbieten normal faults [Lemeille et al., 1999b; Fach in Figure 10] and Basel–Reinach fault (BRF) [Meghraoui et al., 2001; FBalR in Figure 10] are marked by E-facing fault escarpments.

The instrumental seismicity in the graben is relatively moderate with respect to other continental active rifts [e.g. Ahorner, 1983], see detailed information in Doubre et al. [2021].

URG is characterized by a dense historical seismicity with more than 20 earthquakes having intensity higher than VI MSK [e.g. Doubre et al., 2021]. It is most pronounced along both Rhine valley edges [Ahorner, 1983], in agreement with instrumental seismicity, except for the Strasbourg–Karlsruhe segment (RRF-5 Figure 10), where instrumental seismicity is weak [Bonjer et al., 1984]. The historical Basel earthquake (18/10/1356, I_0 = IX, M_w ∼ 6.5) in FCAT, [e.g., Manchuel et al., 2018], M_w = 6.9 ± 0.2 [Barth et al., 2015, Fäh et al., 2009], the largest reported earthquakes during the last millennium in Western Europe, occurred at the southernmost tip of the graben. This earthquake has been a very destruc-

tive event that occurred in the most tectonically active URG, where several faults are considered as active, i.e., the Black Forest, the Rhine, the BRF, and the northern Jura Front Fault [Jomard et al., 2017]. The Remiremont (12/5/1682, I_0 = VIII, M_w ∼ 6.3) and the Mulhouse earthquakes (1/6/1372, I_0 = VII, M_w ∼ 5.6) occurred in the Vosges massif and in the Jura front, respectively. The Wissembourg earthquake sequence (from 29/09/1952 to 10/10/1952 with maximum intensity of VI–VII—Sisfrance) took place near the Riedseltz–Landau Fault (FRhW-5 in Figure 10). Some seismic crises are also identified in the Black Forest Massif. Most of the historical and instrumental events appear to be located on basement faults. Indeed, the average depth of instrumental earthquakes is between 12 and 18 km, with a maximum depth of 25 km corresponding to the Moho boundary [Anikiev et al., 2020].

In conclusion, the URG active faults, anchored in the basement, can be classified into two different categories: (1) N to NNE-trending faults bordering the graben (Rhine West Fault—FRhW in Figure 10, and Vosges Fault—Fvos—in the west and Black Forest Fault in the east) and some faults located inside the graben (RRF, FAch) and, (2) in the southern region, E- to ENE-trending blind inherited Variscan faults. The associated seismicity is mainly located in the basement with an average depth of about 15 km.

3.3.1. *Paleoseismicity studies in the URG*

The Rhine graben is the region (Figure 9) that has been the most extensively studied for paleoseismological purposes since the 1990s, with 14 paleoseismic trenches [Hürtgen, 2017, Hürtgen et al., 2020] (see Table A1), the most recent ones are located on the eastern border fault in the Karlsruhe area, near Ettlingen town [Reicherter et al., 2020, Ritz et al., 2021a].

These studies were performed using multidisciplinary approaches such as geomorphic, geophysics (ERT, HR seismic reflection, GPR, . . .), geological analyses (including borehole) and dating (OSL, TL, ^{14}C, . . .). Most of the studies identified possible co-seismic slips on normal faults associated with vertical slip rates ranging from 0.1 to 0.3 mm/yr. The minimal potential M_w magnitude associated with the studied faults is M_w ∼ 6.5 depending on the segment length [based on scaling laws, i.e., Wells and Coppersmith, 1994, Leonard, 2010].
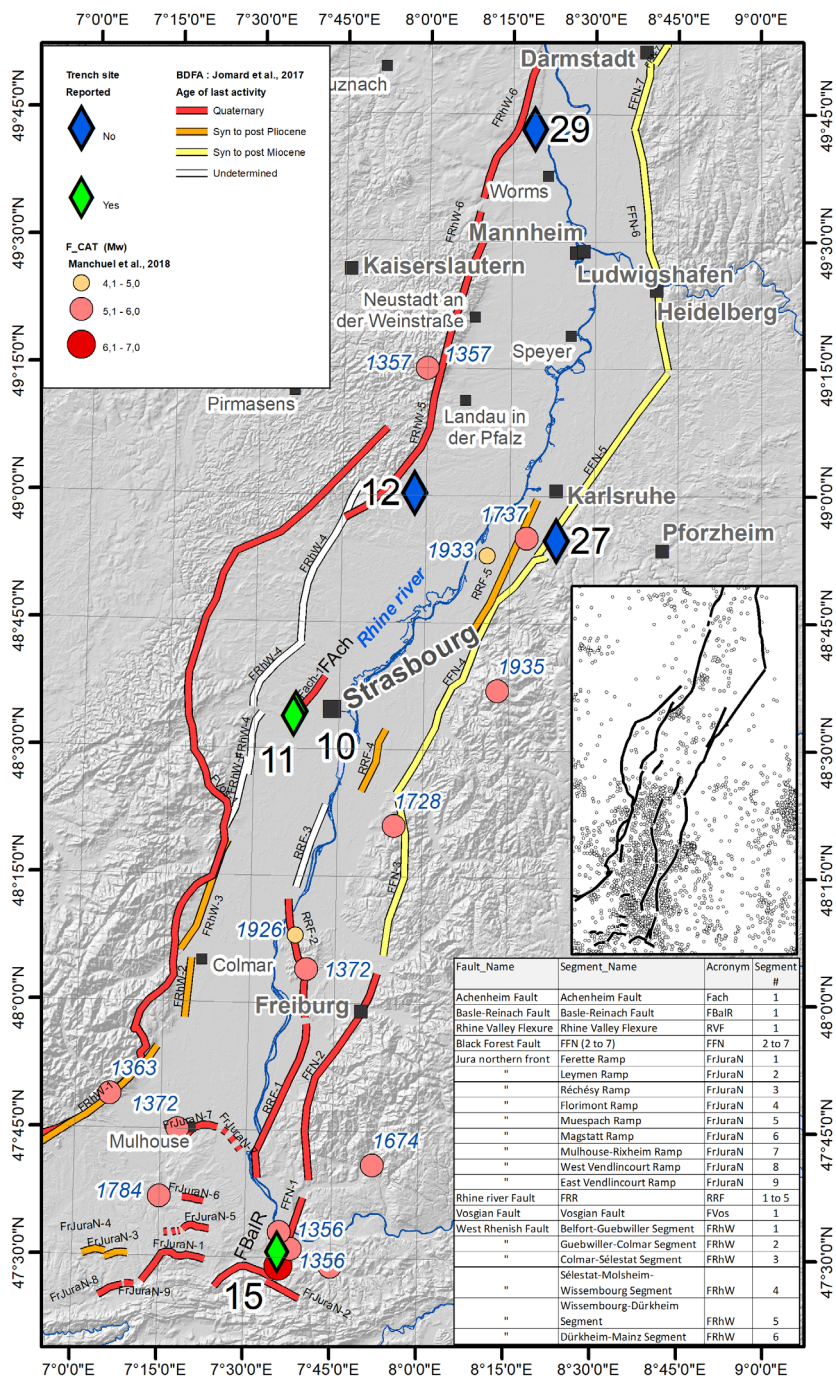
Figure 10. Trench site locations excavated in the URG. Historical and instrumental seismicity from F Cat Catalog [Manchuel et al., 2018] with $M_w > 4$. BDFA reports potentially active faults [Jomard et al., 2017]. Fault names from BDFA [Jomard et al., 2017]: fault name + segment number or name are explained in the table in the lower right corner. The inset map shows instrumental seismicity pattern (CEA/LDG + Si-Hex [Cara et al., 2015] catalogs) without magnitude information and main faults. The DEM in background from (IGN, 50 m for France Territory, NASA STRM, 30 m for Germany, swissALTI3D DEM for Switzerland, 2 m). Trench numbers correspond to sites detailed in Figure 2.
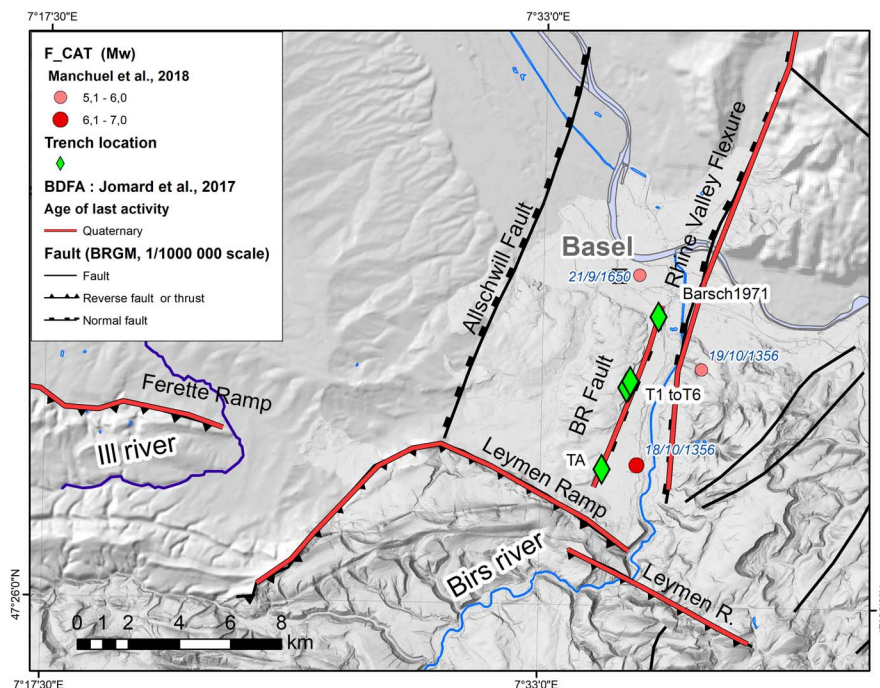
Figure 11. Detailed map of the Basel area showing trench locations from Meghraoui et al. [2001] and Ferry et al. [2005]. The DEM in background derived from IGN, 50 m for France Territory, NASA STRM, 30 m for Germany, swissALTI3D DEM for Switzerland, 2 m. Trench numbers correspond to sites detailed in Figure 2.

We report two trenching sites performed across the Reinach–Basel Fault [Ferry et al., 2005, Meghraoui et al., 2001], and the Achenheim–Hangenbieten slope west of Strasbourg [Lemeille et al., 1999b] that are representative of most comprehensive studies performed within or close to the French URG.

The Basel–Reinach Fault. The 8 km long, BRF (BRF, FbalR in the BDFA, Figure 10 and BRF in Figure 11) is located south of Basel between the Rhine graben and the Jura front and is considered as one of the potential sources of the 1356 Basel earthquake [Ferry et al., 2005, Meghraoui et al., 2001]. The BRF trace is located at the base of the western slope of the Birs valley while the eastern slope of this valley corresponds to the W-facing Rhine Valley flexure (Figure 11). This western slope of the Birs valley should correspond to the BRF escarpment as it is parallel to the regional NNE-trending Rhine graben and has a staircase morphology suggesting a progressive uplift during the Upper Quaternary [Meghraoui et al., 2001]. The fault is locally interrupted by an old meander slightly perched that could have locally erased the

fault geomorphic expression (including the 1356 associated offset) [Ferry et al., 2005]. The BRF probably extends further north and south [Meghraoui et al., 2001], reaching a length of 11–15 km [Ferry et al., 2005]. Based on trenches and seismic section analyses, Ferry et al. [2005] proposed that the BRF is connected at depth to a steep east-dipping normal fault which would be a splay of the major W-facing flexure (Rhine Valley Flexure). Consequently, it has been assumed to be a crustal-scale fault (12–20 km) [Ferry et al., 2005]. The instrumental seismicity in its vicinity displays evidence for event depths of about 10 km.

Paleoseismological investigations on the Basel–Reinach Fault. Several trenches (Figure 11) have been dug in the alluvial series (associated with the ancient Birs river courses) bordering the Bruderholz escarpment (western slope of the Birs valley), where Upper Pleistocene and Holocene are affected by normal faults [Meghraoui et al., 2001]. Fifty four ^{14}C and thermoluminescence dating were performed. Six trenches excavated [Ferry et al., 2005,

Meghraoui et al., 2001] display normal faulting and permit the determination of three coseismic movements of 0.5–0.8 m for a cumulated vertical offset of 1.8 m since 7800 yr. The associated earthquakes are estimated to have globally the same magnitude of about $M_w = 6.9 \pm 0.5$. The most recently recognized event would correspond to the 1356 earthquake. A total of five events were evidenced during the last 13,200 yr suggesting, for late Pleistocene–Holocene period, a recurrence interval of 2500 yr for large to moderate earthquakes. The uplift rate deduced from the dated Quaternary terraces yield a Holocene uplift rate of ~0.27 mm/yr. The uplift rate for the whole Pleistocene is estimated to be about 0.1 mm/yr.

Discussion on the paleoseismic origin of the Reinach faulting. The BRF activity remains controversial as some authors suggest that the fault morphologies observed at the surface are the result of gravitational processes [Laubscher, 2008, Ustaszewski and Schmid, 2007]. Observations at some trenches appear to correspond to progressive deformation that would more likely be related with slope instability associated with the concavely shaped slope base caused by active meandering erosional process of the Birs River during the end of the LGM or Holocene floodings (personnal observations). Other authors [Lambert et al., 2005, Meyer et al., 1994] argued that the macroseismic data of the Basel earthquake are more compatible with an earthquake occurring on an E-trending fault than a N-trending fault as the BRF. Reassessing the Basel earthquake characteristics, Fäh et al. [2009] concluded that it is impossible to clearly identify the 1356 earthquake source: the Rhine Graben Fault system or the Rhine–Bresse transfer zone. They pointed out that both fault systems cross the epicenter area, and consequently can be both the potential 1356 source. In addition, Fäh et al. [2009] indicated that calculating the BRF's expected slip using the best regional stress tensor [Plenefisch and Bonjer, 1997] would yield a mechanism with a minor normal and a dominant left-lateral faulting component that is not evidenced by Ferry et al. [2005] and Meghraoui et al. [2001]. Finally, even if the ruptures on the BRF would correspond to slope instabilities, these could have been triggered by a strong shaking generated by an earthquake like the 1356 Basel one, occurring on a blind structure at depth, so these paleoseismic observations could pro-

vide an indirect calendar for destructive earthquakes in the Basel area.

The Achenheim–Hangenbieten escarpment. The Achenheim Fault (AF, Fach in BDFA, Figures 10, 12C) was originally observed by Wernert [1957] as a 160 m long feature exposed on the floor of the Achenheim quarry [Lemeille et al., 1999b]. A 1 m deep superficial depression was also observed at the top of the quarry above this fault outcrop. Subsequently, this fault position was defined from geomorphological, seismotectonic, geophysical and sedimentological studies [Lemeille et al., 1999b]. A proposed fault trace [BDFA, 2020, Jomard et al., 2017] was expected to extend northward on the basis of hydrographic anomalies displayed on the DEM around Mundolsheim (Figure 12C). It may also extend southward since the Bruche River terrace shows a morphological slope of about 5 m in the southern prolongation of the Achenheim scarp [Figure 12D; Lemeille et al., 1999b]. With this potential extent, a maximum length of approximately 15 km has been proposed for a ~N-trending, 70°–50°-E-dipping normal fault with a minor left-lateral component [Baize et al., 2002].

Paleoseismological studies at Hangenbieten and Achenheim. Two trenches were dug across the fault trace at Achenheim and at Hangenbieten (Figures 12A and 12B). At Achenheim, a major N05° E-trending, 70° E-dipping fault with a 6 m normal apparent offset affects the whole sequence exposed in the trench (Middle Pleistocene −150 to 300 ka, the most recent being dated at 27 ka) [Lemeille et al., 1999b, Baize et al., 2002].

At Hangenbieten, another trench displays evidence for a 16 m vertical offset affecting a sandy level dated at 370 ka on a N50° E-trending, SE-dipping normal fault. A rooting of the structure as an antithetic of the main westward-dipping fault seen on seismic reflection image (Figure 12E), based on subsurface seismic survey and a potential seismic event with M_w ranging from 6.0 to 6.5 has been proposed [Lemeille et al., 1999b]. Slip rates of about 0.03 mm/yr and 0.04 mm/yr have been estimated from offsets dated with ^{14}C and thermoluminescence at Achenheim and Hangenbieten, respectively [Lemeille et al., 1999b].

Discussion about the paleoseismic origin of the Achenheim–Hangenbieten escarpment. A seismic
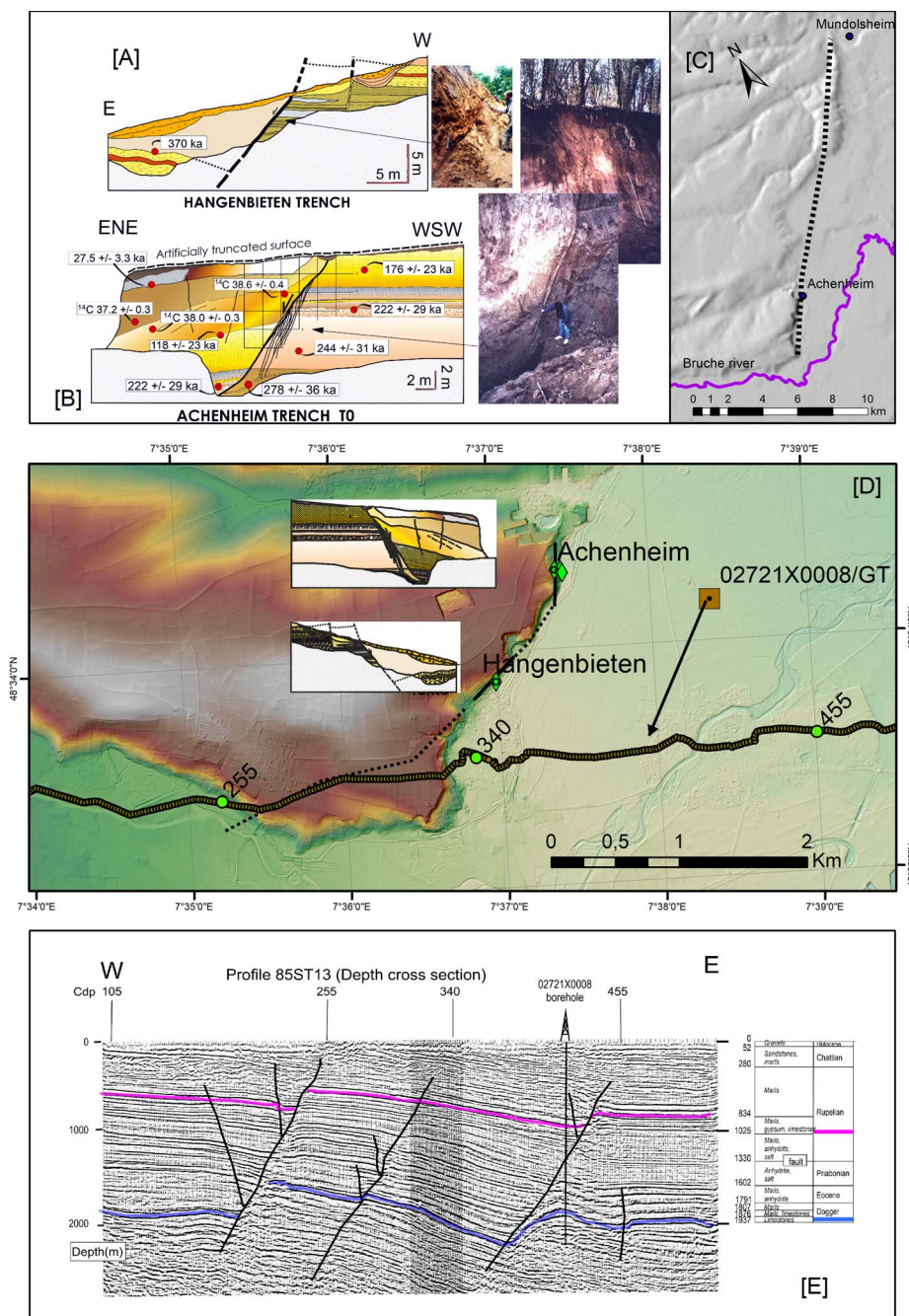
Figure 12. (A) Logs and pictures of Achenheim and (B) Hangenbieten trenches. Thermoluminescence dating come from Buraczynski and Butrym [1984] cited in Lemeille et al. [1999a]. ^{14}C dating are specifically indicated. (C) Inset map locating the BDFA FAch fault (dotted line) with respect to Achenheim–Mundolsheim slopes. (D) DEM (1 m resolution, IGN) and location of the seismic section 85ST13. Simplified logs of trenches are drawn with respect to the geographic position (east on the right). The borehole 02721X0008 (accessed on the BRGM/BSS website) is projected on the seismic line trace with respect to the major fault strikes (NNE-striking as seen on GEORG project (see http://maps.geopotenziale.eu/?lang=en). (E) Seismic profile 85ST13 and correspondence between the borehole geology and the seismic section. Two specific reflectors have been drawn in order to show the overall structure. Blue could correspond to the "Grande Oolithe" limestone facies and purple to a reflector located above the Oligocene salt layers. The fault identified in the borehole may correspond to one of the west-dipping faults displayed on the section. The fault located near CDP 255 or 340 could be connected to Achenheim and Hangenbieten faulting evidences that however show east-dipping faulting (antithetic fault associated to main faults).

reflection section perpendicular to the AF and crossing through the Hangenbieten scarp shows at depth 50° W-dipping major normal faults opposite to the dip of the AF observed at the surface. These faults offset the Dogger and Oligocene reflectors by about 200 m and extend downward into the basement. They are associated with minor antithetical east-dipping faults which may be associated with either a half-graben, or a negative flower structure in the case of a purely normal faulting or of a transtensional tectonic regime, respectively. The proposed 15 km long AF could then be associated with one of these west-dipping structures. The scarp would thus have been created by the lowering of the hanging wall over the antithetic east-dipping fault.

The analysis presented suggests an Achenheim Quaternary fault activity that could be linked to a structure at depth. This fault presents a normal faulting with a left-lateral component with rates ranging between 0.027 and 0.045 mm/yr since the Middle Pleistocene. Nevertheless, the geometric relationships between surface and deep geophysical observations have still to be more robustly established. Alternatively, the deformation observed at the surface could be interpreted as resulting from gravitational processes (i.e., slope destabilization in the loess and Saalian sands due to Rhine river scouring).

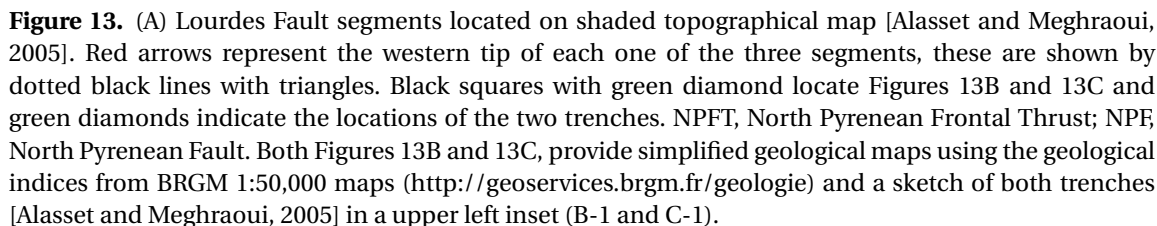### 3.4. *Seismotectonic setting of the central–western Pyrenees*

The Pyrenees mountain range corresponds to an asymmetric orogen where the major foreland basin, the Ebro basin, is located to the south. Shortening in the Ebro and Aquitaine basins stopped by the Early Miocene. From Early–Mid Miocene until now, the stress regime in the Pyrenees appears confusing and is still a matter of debate [e.g. Sylvander et al., 2021]. There are clear lines of evidence for normal faulting during Neogene and Quaternary, which is coeval to a significant uplift of the Pyrenees range, especially along the axial zone [Calvet, 1996, Lacan and Ortuño, 2012] and in the Eastern Pyrenees [Lacan and Ortuño, 2012]. At several places, it may be difficult to separate the contribution of Quaternary normal faults from the Neogene ones [Lacan and Ortuño, 2012]. Conversely, the evidence for Quaternary reverse faulting appears weaker at several locations where reverse faults or folds are seen

affecting Pliocene or Quaternary series. Indeed, a non-tectonic origin cannot be discarded [see discussion in Lacan and Ortuño, 2012, Baize et al., 2002]. Nevertheless, in the Pyrenees there have been several destructive historical earthquakes [1373, 1427, 1428, 1660 with I ≥ VIII, FCAT, Manchuel et al., 2018, see Figure 2] and many instrumental earthquakes have been recorded [Souriau et al., 2014]. The 22 best-constrained focal mechanisms in the Pyrenees, from event magnitudes in the range 3.9–5 and focal depths between 8–10 km exhibit normal faulting solutions [Chevrot et al., 2011, de Vicente et al., 2008, Souriau et al., 2014, Sylvander et al., 2021]. Four solutions correspond to strike-slip faulting and all mechanisms combined may agree with a transtensional stress regime. Nevertheless, the central axial zone and eastern French Pyrenees are void of well-constrained focal solutions so that the seismological data do not permit to determine the stress regime in these regions. Finally, GPS data do not measure any significant movement across the Pyrenees. According to Nocquet [2012] this geodetic rate of deformation should be below 0.2 mm/yr. Nonetheless, the processing of GPS data [Asensio et al., 2012, Nocquet, 2012, Rigo et al., 2015] suggests that the Pyrenees stress regime should be extensional, at least in its western part [Sylvander et al., 2021].

In conclusion, seismological and geological data suggest the present-day stress regime of most of the Pyrenees is characterized overall by normal faulting, associated with very low strain rate. In the central and western Pyrenees where the "Lourdes Fault" is located, the seismic foci display a north-dipping seismic zone limited to the south by the North Pyrenees Fault where there is active normal faulting.

3.4.1. *The "Lourdes Fault"*

The "Lourdes Fault" (Figure 13A) is defined as an E-trending, N-dipping, reverse fault that extends from central to western Pyrenees along some 50 km [Alasset, 2005, Alasset and Meghraoui, 2005]. Overall, it appears identified, between Lourdes and Oloron–Sainte-Marie, on the basis of an E-striking microseismicity belt (see previous paragraph) and at the more local scale its topographical signature could correspond to E-trending elongated depressions (Lourdes, Capbis, and Ourtau valley east of Saint Christau), which are located at the toe of the northern topographical front of the Pyrenees. Hence, the

Figure 13. (A) Lourdes Fault segments located on shaded topographical map [Alasset and Meghraoui, 2005]. Red arrows represent the western tip of each one of the three segments, these are shown by dotted black lines with triangles. Black squares with green diamond locate Figures 13B and 13C and green diamonds indicate the locations of the two trenches. NPFT, North Pyrenean Frontal Thrust; NPF, North Pyrenean Fault. Both Figures 13B and 13C, provide simplified geological maps using the geological indices from BRGM 1:50,000 maps (http://geoservices.brgm.fr/geologie) and a sketch of both trenches [Alasset and Meghraoui, 2005] in a upper left inset (B-1 and C-1).

northern edges of these depressions were interpreted as the south-facing escarpment of the Lourdes reverse Fault. However, the reverse displacement cumulated on the "Lourdes Fault" should be very small and opposite to the Pyrenees topography, as displayed on Alasset and Meghraoui's figures [2005]. Moreover, the alluvial terraces seen on both sides of these elongated valleys are observed at a similar elevation, indicating that the Lourdes Fault should be a very young fault [Neopal report, 2008]. The possibility for a young reverse fault is precluded by the normal faulting focal mechanisms [Chevrot et al., 2011, Souriau et al., 2014, Sylvander et al., 2021] in the vicinity of the "Lourdes Fault". Thus, the reverse "Lourdes Fault" is very weakly identified because an E-trending fault in this area is expected to have a normal dip-slip component. Two exploratory trench

sites were analyzed to perform paleoseismic observations: Arcizac and Capbis [for more details, see Alasset and Meghraoui, 2005, Neopal report, 2008].

Paleoseismological investigations in the Arcizac area. Arcizac site is located NE of the Lourdes depression (Figure 13). The trench was located at the contact between the base of a steep slope (≥30°) and a lower terrace of the Graves or Echez creek. The trench log redrawn from Alasset and Meghraoui [2005] (Figure 13B) displayed 40°–45° S-dipping conglomerates (Mcg in Figure 13B; ^{14}C ages ranging from ~11,240 BC [calibrated date] to ~40,450 BP [conventional age]) overlying a 20° N-dipping shear zone interpreted as a reverse fault thrusting southward on younger alluvial conglomerates (Rch in Figure 13B; ^{14}C Ca ~ [4221–3094] BC). The shear zone exposes clay fabric

and a silty-sand unit with oriented gravels and pebbles dipping ~25 north. This reverse fault is sealed by colluvium (Ccg in Figure 13; ^{14}C Ca [2398–2038] BC). This sealing horizon is interpreted as the event horizon of an earthquake, which would have occurred between 4221 and 2038 BC [from 2σ calibrated age: Alasset and Meghraoui, 2005, Alasset, 2005]. According to another interpretation [Neopal report, 2008], this "event horizon" corresponds to the lower part of a landslide event originating from the unstable steep slope and favored by the morainic and fluvio-glacial nature of its material. Indeed, this steep slope corresponds to the inner frontal moraine of the Lourdes glacier ending during the Last Glacial event.

Paleoseismological investigations in the Capbis area. Capbis site is located at the Bourda hamlet on the northern side of the Capbis depression (Figure 13C). The trench was located at the contact between a S-dipping slope carved within Cenomanian flyschs and a lower terrace of a local creek. The trench log [Alasset and Meghraoui, 2005, Alasset, 2005] shows a 55°–70° S-dipping contact between the Cenomanian flyschs and alluvial deposits (^{14}C ranging from 19,040 ± 930 BP to 6370 ± 50 BP). The former deposits are covered by colluvium (^{14}C ranging from 4520 ± 100 BP to 3760 ± 60 BP) so that the base of this colluvial deposits is interpreted as the event horizon of an earthquake, which would have occurred between 5388 BC and 2918 BC (from 2σ calibrated age). According to Alasset and Meghraoui [2005] and Alasset [2005] this normal surface rupture would result from a near-surface shallowing dip of the reverse "Lourdes Fault". However, the published material does not permit to discard the possibility that the steep contact between the flyschs and the alluvial deposits could result from the lateral erosion of the creek channel during the Holocene [Neopal report, 2008]. Thus, further paleoseismic investigations are needed to determine whether the steep contact corresponds to a coseismic rupture on a small normal fault of the North Pyrenees seismic zone or to creek lateral erosion. In conclusion, both trenches provide interesting information, but unfortunately alternative options were not contemplated in the published literature. The Capbis trench could correspond to an earthquake surface rupture while the Arcizac reverse fault disagrees strongly with all the recently published seismological data (see above), hence it should

better result from the unstable nature of the steep slope overhanging the trench site to the north. This slope instability should be included in any hazard plan for development prospect of the Lourdes area.

4. Discussion

4.1. *Is paleoseismology suitable in low-seismicity regions?*

Paleoseismology was initially developed in regions where faults are well identified and often associated with significant seismicity, such as in California where destructive earthquakes have occurred but where few, if any, older historical earthquakes are known. Seismicity of metropolitan France is significantly different and thus one could question the use of this methodology in Western Europe. Some thirty years of paleoseismology permit to propose some balanced answer. If we could compare the number of trenches dug with respect to the amount of "significant" results, the benefit-cost ratio would not favor using trench paleoseismology in France. However, such a rather negative answer deserves to be carefully analyzed from two perspectives. The former is more developed below in the next subsection on the pitfalls; it shows that the "California" approach was not appropriate to be directly transferred to metropolitan France. The second perspective considers that the paleoseismicity approach can be adapted to the seismicity setting of Western Europe. This adaptation is still going on, nonetheless it is already a rather powerful approach, although time consuming and difficult to implement, but able to complement the seismicity catalogs (instrumental and historical). This will be discussed in the subsection dealing with the results brought by the paleoseismicity approach in France.

4.2. *The pitfalls of a limited paleoseismic approach*

In the 1990s, due to the lack of an adapted methodology and on the basis of descriptions of deformational evidences, paleoseismic exploratory trenches were often carried out with very limited or even no preliminary investigations aimed at clarifying the relationship between the structures observed at the surface and the major faults. Sometimes, on the basis of a rapid morphological approach, faults have been identified as potentially active without robust lines

of evidence. As a result, it has often been difficult or even impossible to establish the size, timing, and frequency of the inferred paleoseismic event (i.e. linking the fault size to seismic scenarios).

Furthermore, the dating issue has often been very poorly addressed (no radiochronology or thermoluminescence/OSL dating). At many sites there was just a very rough dating based on arguable stratigraphic correlations based on often indirect stratigraphic considerations (facies, terrace elevations, archaeological artifacts...) leading to very broad hypotheses (i.e., the Courthézon Fault broke once or twice between the "Riss" and the "present" [Combes et al., 1993]). Nevertheless, as soon as some deformation evidences have been found and subsequently studied, the kind of process that created the Quaternary deformation was only contemplated within a seismotectonic perspective.

At several sites the tectonic origin was not confronted with other alternatives (sedimentary, glacial, solifluction, gravity effects, landslide, etc.) that should have been raised. This problem was stressed in the early synthesis on French paleoseismic studies [Sébrier et al., 1997]. This a posteriori approach has been sometimes implemented trying to link the structures observed at the surface to deep faults, in particular by reinterpreting seismic profiles from oil exploration or by carrying out higher resolution seismic profiles (e.g., MDF: Valvéranne and Forestière trenches [Cushing et al., 2008], AF: Hangenbieten [Lemeille et al., 1999b], Courthézon Fault with discussion on the FSH seismic profile 80 SE 4B [Combes and Carbon, 1997]). In the above-mentioned studies, there was often no clear link between the location of the deep faults and the surface observations, introducing a doubt on the tectonic origin of the observed Quaternary deformations, or at least on the structural relationship between the surface faulting and the deep structures potentially capable of generating significant earthquakes that could produce the "surface ruptures". Alternative hypotheses were proposed for Courthézon (Oligocene salt creep-induced deformation), Achenheim, (loess slope instability resulting from the lateral erosion of an old bed of the Rhine river), Valvéranne (bedding slip associated with active folding induced by a secondary segment of the MDF).

An extreme case is provided in the Aube department in the Paris Basin where a well-exposed outcrop with very clear surface deformation affecting the Quaternary raised the question of the possible earthquake occurrence in this region which is considered to be tectonically inactive [Baize et al., 2002, 2007, Van Vliet-Lanoë et al., 2019]. The detailed sedimentological analysis, the examination of the paleoclimatic setting permitted to establish a cryogenic origin of the deformation affecting the chalk. This was confirmed by the seismic section analysis, which did not provide evidence for any deep structure rooting of the observed surface deformation.

4.3. *Results brought by paleoseismology in metropolitan France: toward a paleoseismic approach for low-seismicity regions*

Several works reported in this publication provide arguable results because the analyzed active fault was not robustly identified. This was one of the major efforts and final recommendation of the European SAFE project (2004). A lot of efforts have been made in the western European paleoseismology community to *improve active fault identification.* Even if the gap is not entirely filled, most of the European active tectonic researchers are aware of this problem. Basically, a good fault identification needs to integrate the faulting information at different scales from local to regional, as well as from the surface down to a depth of several hundreds of meters and up to several kilometers and reconcile this with all the available information on seismicity. For instance, to find surface rupture associated with the Trévaresse Fault (1909 Aix-en-Provence earthquake), several exploratory trenches were performed at the topographic "scarp" and all of them exhibited Oligocene–Miocene vertical bedding without any surface fault rupture [Nguyen et al., 2007, Chardon et al., 2005, 2009]. Thus, the expected reverse fault was either blind or has propagated farther south, within the foreland. To test this second hypothesis microtopographic analysis was conducted south of the main topographic "scarp" to find the subdued topographic slope gradient associated with the expected emergence of a southward propagating reverse fault. This permitted to obtain one of the best results provided by a paleoseismic approach in France (see above Section 3.1.1). Several episodes of fault rupturing the surface south of the Trévaresse ranges do indicate that *surface rupturing earthquakes repeat on*

the same fault even in a low-seismicity area. At least some low-seismicity fault behaviors are somewhat comparable with that of high seismicity ones even if the mean return period is obviously much lower.

Sometimes a better fault identification thanks to the reinterpretation of seismic lines allows a reappraisal of previously published results. This is the case of the Valvéranne site, where the Quaternary deformation was initially interpreted as the upward dying out of a near-surface fault rupture (see above Section 3.1.3). Later on, this fault was considered as secondary because it is antithetic with respect to the two major faults observed on a seismic line. Then, the Valvéranne deformation [Ghafiri, 1995, Sébrier et al., 1997] was reinterpreted as a bedding slip rupture amortizing within the Upper Pleistocene sediments [Baize et al., 2002]. Such bedding slip indicates folding associated with displacement on the MDF similar to some structural observations made on other reverse faults [Tapponnier et al., 1990, Kelsey et al., 2008]. The amplitude of the bedding slip suggests this should correspond to earthquake magnitude $M_w >$ 6. Thus, a low-seismicity fault may produce *paleoearthquakes big enough to be associated with bedding slip ruptures.*

Therefore, paleoseismicity studies in low-seismicity regions need to use a multidisciplinary approach combining all the available methodologies: geophysical, morphometric, morphotectonic, high-resolution DEM and LiDaR imaging methods, dating permitting to improve the fault characterization and location at a resolution that is high enough for the use of paleoseismology in low-seismicity regions. Studies carried out in the early 2000s have successfully begun to integrate the progressive approach based on combined geology, geophysics and geomorphology [i.e., Trevaresse Fault: Chardon and Bellier, 2003, Chardon et al., 2005, 2009].

The best-constrained slip rate estimates obtained by paleoseismic observations and dating are very low, ranging approximately between 0.01 and 0.1 mm/yr, while the highest subsidence rates estimated from Quaternary thickness in the northern URG, are between 0.1–0.2 mm/yr. As the major surface rupturing earthquakes have estimated magnitudes of $M_w \geq 6$, the approximate loading time needed for accumulating 30–50 cm of potential slip on a fault is in the range of 10–30 ka. Hence, these surface rupturing earthquakes should not be frequent or in other words

have long recurrence intervals. Considering the highest subsidence rates, the recurrence intervals may be somewhat shorter but still in the range of 5 to 10 ka. These time intervals are obviously far beyond the reach of instrumental or historical seismic records and have direct consequences on the hazard assessment in France. In addition, since the climatic conditions during the above estimated time intervals can be highly erosive in France [Siame et al., 2004], this rather *infrequent occurrence of destructive* ($M_w > 6$) *earthquakes does not favor preserving fault rupture evidences in the landscape and explains very subdued tectonic signal in the topography.*

Indeed, the morphological signature of a fault is one of the indicators that may suggest that there is a possible seismogenic potential on this fault. For instance, the Vuache Fault at the origin of the 1996 Annecy earthquake [Thouvenot et al., 1998] displays a clear morphological signal such an alignment of 200–300 m long left-lateral talweg incised in Quaternary sediments (see Section 3.2.1).

4.4. *Potential for surface faulting associated with significant earthquakes in metropolitan France*

Although slip rates of active faults are very low (on the order of 0.1 mm/yr, see above) some active fault systems are known to be able to host rare but significant earthquakes such as the Rhine Graben Faults (both borders and internal basin faults), some western Alps faults (Higher Durance, Belledone), Frontal external Alps or Pyrenees faults (North Pyrenean zone, MDF and western Provence E-trending thrusts). In old Paleozoic rocks, some major crustal faults (long and rooted) are also prone to rarely produce significant earthquakes such as the frontal zone of Hercynian orogeny [North Artois-shear zone: Jomard et al., 2017, García-Moreno et al., 2019] probably associated with the $M_w \sim 6$, earthquake of 1580, or the Sillon Houiller Fault zone in western Massif Central (several hundred km long, see location on Figure 2), or the South Armorican shear zone in Brittany, where no paleoseismic evidence has been found although some Quaternary deformations have been mentioned [Baize et al., 2002, Kaub, 2019], and one of the strongest historical earthquake reported in metropolitan France (1799 Bouin earthquake, $M_w \sim 6$, see location on Figure 2).

4.5. *Questions remaining to be solved*

The origin of seismogenic deformation in France remains a matter of debate. For example, the 2019 November 11th, M_w 4.9 damaging earthquake near Le Teil (see Figure 3 [28] for location) raises the question of seismic loading and seismic source that can trigger such a shallow event in very slow deformation settings and on previously unruptured faults, even if this fault was geologically mapped [the Rouvière Fault, Ritz et al., 2020]. It also questions the seismogenic behavior and the concept of seismic cycle in such settings. Indeed, *two models are available to account for the seismogenic behavior* in metropolitan France: (1) the "classical" model of the seismic cycle, which is characterized by the tectonic loading between two events on the same fault, and (2) the model for stable continental regions [Calais et al., 2016] that considers the tectonic loading in continental interiors to be too small to permit reaching the seismic rupture on a fault; in such a model, earthquakes do not repeat on the same fault because the far field stresses maintain the continental lithosphere close to rupture, hence transient local stress variation on a fault may lead to seismic rupture. Thus, this model 2 could explain the Le Teil earthquake specially if it is the first time that the small Rouvière Fault ruptured with a reverse slip. It permits to understand how a fault generates a big quake only once.

Concerning the seismic cycle (model 1) it can apply to the slow-slipping Trévaresse Fault, as there are lines of evidence (see Section 3.1.1) that earthquakes repeat on this fault and possibly even with similar ruptures suggesting that their mode of recurrence could correspond to the characteristic earthquake [McCalpin, 2009]. For sure, many more studied sites are needed to be more conclusive on the model that applies to other active faults in metropolitan France, even if we are aware that the anticipated long return period on a given fault does not favor preserving long records of datable earthquakes at a site. This might be one of the major limitations for using the paleoseismic approach in metropolitan France.

An important legacy of the 1996 Annecy earthquake (see Section 3.2.1) is that for the first time in France a seismic surface rupture may have been observed after an earthquake located on a known major fault. Nevertheless, the most interesting point is that this surface rupture was produced by a $M_\mathrm{w} = 4.9 \pm 0.3$

[FCAT in Manchuel et al., 2018] event, although the damage (Io = VII) was important for such a small magnitude. Nevertheless, a paleoseismic study did not permit to find any clear evidence of surface rupture. Thus, this small relatively destructive event clearly displays that even *small earthquakes can be harmful.* Furthermore, the Maragrate Fault (see Provence Section 3.1.3) permits to question the hazard of short faults. More recently, the Teil earthquake was some kind of electroshock that made the fault geologists, who were working on the large active faults, realize that the local risk, even on "small" faults, cannot be neglected within the low-seismicity territory, like France. This increases the difficulty to identifying these *potentially active small faults.* How many faults, like the Rouvière Fault, that are a few kilometers long, do not affect recent deposits, and do not have a significant morphological signature? The answer is: hundreds of thousands in the most active regions of metropolitan France. Are the methods mentioned above enough? The challenge is set up! In such a case, the paleoseismic approach can hardly be used to *characterize the hazard on small-length faults* because the goal *is probably beyond the detection threshold of surface rupture that can be determined with trench observations.* The detection threshold of an earthquake rupture using paleoseismic analyses was estimated during several years as M_w 6, [McCalpin, 2009], today it is considered that the paleoseismic approach does permit to find surface rupture for earthquakes with M_w 4.9 [see discussion in Ritz et al., 2020]. However, this kind of small rupture (in length and amount of displacement), is a challenge for paleoseismic methods. To date, only recent, superficial (~2–5 < km depth) and moderate (<M_w 6.0) earthquakes (Lambesc $M_\mathrm{w} \sim 6$, Annecy M_w 4.9 ± 0.3, Le Teil M_w 4.9) are associated in France to observed small (<20 cm) surface dislocations.

Finally, *blind faults* have obviously not been considered during the 30 years of paleoseismic studies in metropolitan France. However, some blind faults could correspond to seismogenic sources in France such as the Lambrussier NW-striking anticline [LBF on Figure 3, Hippolyte and Dumont, 2000, Godard et al., 2020] or the Blausasc NNE-trending hidden fault (10 km north of Nice, Figure 2) [Courboulex et al., 2007, Larroque et al., 2021]. On such structures, paleoseismic approach remains obviously limited and can only analyze the secondary evidences

based on morphological approach, dating and/or spatial distribution of microseismicity, conditioned by available and enough dense temporary or permanent seismic network.

5. Conclusions

We have presented a synthesis of the paleoseismic studies, which have been conducted in metropolitan France over the last 30 years. A short summary of the evolution of these studies and a critical analysis of the most interesting ones permit highlighting the strengths and weaknesses of the paleoseismic methodology in France and neighboring areas. Due to the climate of Western Europe during the Late Pleistocene and Holocene (alternating glacial and interglacial periods with strong to weak erosional conditions), high imprint of human activity on the landscape, and low slip rates of active faults, the application of the paleoseismic approach in metropolitan France to identify faults likely to generate destructive earthquakes, is challenging. Many of these paleoseismic studies are confronted with the difficulty of associating Quaternary deformation observed at the surface with a well-identified fault. In too many trench analyses, the fault identification is not robust, although this problem is now better accounted for in most published paleoseismic observations. Indeed, there is not yet a straightforward methodology to address the issue of fault identification; nonetheless, the best results are obtained using a guideline based on a multidisciplinary approach at different scales (e.g. SAFE and Paleosis European projects), from regional (e.g., 20 km–1 km) to local (1 km–1 m).

Paleoseismic studies have permitted to obtain important new results. The most important is that the Trévaresse Fault, the source fault of the $M_w \sim 6$, Provence earthquake of 1909, has generated several earthquakes with surface ruptures observed at the same location. This demonstrates that even in regions of low seismicity and with slow-slipping faults, seismic events can repeat on the same fault. In addition, the displacement per event appears to range between 20 and 30 cm, thus, this reverse fault could fit the characteristic earthquake model. Whatever the model, more data are needed to determine whether this is the common fault behavior in metropolitan France. Data from neighboring countries, indicate that several active faults in Western Europe,

both normal and reverse, produce repeatedly earthquakes even with very low slip rates, on the order of 0.01 mm/yr. Such slip rates indicate that the recurrence interval between two destructive earthquakes should be at least 10–30 ka for $M_w \sim 6$ to permit the corresponding seismic loading, if this behavior model applies. Consequently, such long recurrence intervals do not favor preserving a long record of seismic events at a single paleoseismic site. Hence, only exceptional site conditions will allow to get a long seismic record and thus, the fault behavior model may remain beyond the reach of paleoseismic studies in metropolitan France. Finally, these paleoseismic results clearly display evidence that the historical seismicity is not enough to properly assess seismic hazard in metropolitan France.

Paleoseismic studies were also confronted with ruptures on secondary faults, these are of two different origins: either splays connected with major faults or bedding slip in folds. The first case raises the problem of the source significance with respect to the potential magnitudes associated with surface rupture. There are two faults with such problem in the URG, namely the BRF and the Achenheim–Hangenbieten Faults, where well-identified splays from major normal faults are seen on seismic lines rather than on the major fault. In both cases a non-seismogenic origin for the surface ruptures has been proposed (slope instability), casting questions on the significance of such shallow normal fault ruptures and their implications for the local seismic hazard. In contrast, bedding slip is a more robust indicator of strong seismic events, nonetheless its occurrence is limited. To our knowledge, Valvéranne on the MDF is the only identified site in France with such structural configuration. Bedding slip is considered as a seismogenic source [Kelsey et al., 2008] that corresponds to slip accommodating folding triggered by coseismic slip on a "master ramp fault". It is suggested that "folding earthquakes" are probably in the range of magnitude 6. This agrees with previous magnitude estimates on the MDF [Cushing et al., 2008].

The 2019, M_w 4.9 Le Teil earthquake raises the question of the seismic loading and seismic source dimensions that can trigger such shallow events on faults that have not experienced ruptures during the Late Quaternary [Cornou et al., 2021, Ritz et al., 2020, 2021b]. Thus, faults capable of producing surface ruptures can remain unnoticed. It raises questions

about the seismogenic behavior and the concept of a seismic cycle for such type of faults. Whatever small faults capable of producing $M_w \sim 5$ events can be damaging and even cause surface rupture if their foci are very shallow, as demonstrated by the 1996 Annecy earthquake ($M_w \sim 4.8 \pm 0.5$) and the recent 2019 Le Teil earthquake [Ritz et al., 2020, 2021b]. Obviously, such faults cannot be completely inventoried in the whole metropolitan France, except probably in the vicinity of nuclear and hazardous facilities where specific investigations should be performed.

Paleoseismology can provide important inputs for the seismic hazard assessment such as fault slip rates and return period of destructive earthquakes. These data can be useful both for probabilistic and deterministic seismic hazard assessment [IAEA TECDOC No. 1767, 2015]. The segment rupture dimension assessment highly depends on the fault segment length and its rooting at depth. Segment length permits to estimate the maximum magnitude for a given fault source. A precise chronological framework is needed to quantify seismicity rates and return periods. Identification of paleoruptures at the surface indicates the potential for capable faults and for shallow destructive earthquakes. In addition, precise knowledge of the surface fault trace for major and secondary faults permits to perform a probabilistic fault displacement hazard analysis that allows to assess rupture hazard for critical facilities [i.e., Baize et al., 2020, Nurminen et al., 2020].

Based on our review we formulate four recommendations for future paleoseismic investigations in metropolitan France, or more generally in regions characterized by low slip rates:

- Not all Quaternary deformation seen at the surface, including those inside trenches, are necessarily of tectonic origin, thus, other non-tectonic origins should be considered, and their likelihood evaluated.
- Well-constrained fault identification implies relating convincingly a surface rupture of tectonic origin to a major fault observed on subsurface geophysical imagery. Such fault identification is necessary to assess the source dimensions and hence the potential magnitudes, and the associated seismic hazard.
- Too many paleoseismic events inferred from trench observations were poorly dated, significant efforts have to be made for using

modern dating methods focused on the Quaternary, these must be continued. Indeed, successful dating needs to fulfill three points: (1) a clear identification of the seismic event horizon, (2) a selection of material suitable for dating and contemporaneous with deposition, and (3) to use, if possible, multiple dating methods.

- Blind seismogenic faults are potential sources for seismic hazard. Accounting for these sources imply developing some indirect paleoseismological approaches to better quantify the deformation they can produce at the surface [see e.g., Siame et al., 2015].

Conflicts of interest

Authors have no conflict of interest to declare.

Acknowledgments

Appendix

See Table A1.

Table A1. Available information on the potential paleoseismic trenches performed in France. This provides a summary synthesis of the available information (to our knowledge) on paleoseismic trenches excavated in and close to metropolitan France. The information filling this table corresponds to the one given by the authors in their reports, dissertation thesis, as well as "gray" and published scientific papers and is not necessarily endorsed by the authors of this summary synthesis

Trench site name	Fault system	Date	Operator/ funding	Report/ thesis	Dating or stratigraphic attribution	Nb trenches	Works	Log	Boreholes	Geoph methods	Available seismic réflexion profile	EQ event(s)/ other	Published paper(s) and/data base	Trench location: [Trench number] (longitude; latitude) DDD.ddddd
Estavar	Tet fault	1990–1992	IPSN/ GEOTER	Unpublished report	No, Stratigraphic correlation (SC)	1	Trenching	Yes Baize et al. [2002]		Yes	No	Reverse tectonics or gravitational (preferred)	Baize et al. [2002]	2.00957196; 42.46270463
Valveranne	MDF	1991	BRGM/ UPVI	Ghafiri [1995]	Yes (¹⁴C)	1	Trenching	Yes			Yes (IFP, Total reports, CEA reprocessing)	≥1	Sébrier et al. [1997], Baize et al. [2002], Siame et al. [2004]	5.79956456; 43.85062273
Baumont de Pertuis	MDF	1992 (?)	IPSN/ GEOTER	IPSN/GEOTER unpublished report	Yes (¹⁴C), too recent	1	Trenching	Yes			Yes (IFP, total reports, CEA reprocessing)	0 Truncated?	Grellet et al. [1995]	5.68013116; 43.72395867
Couthezon (Latour)	Nimes F	1992	IPSN/ GEOTER	Unpublished report (GEOTER)	?/analog facies. tiles	2	Trenching	Yes			FSH seismic profile interpretation in ANDRA. 1997	≥1	Combes et al. [1993], Carbon et al. [1993], Baize et al. [2002]	T1: 4.87144760; 44.09489180 T2: 4.87118632; 44.09524938
Meilhan	Blind reverse thrust (Campagne Anticline)— associated to diapirism	1993	IPSN/ GEOTER	IPSN/GEOTER unpublished report	No. SC	1	Outcrop cleaning	Yes				≥2	Carbon et al. [1995], Baize et al. [2002]	−0.70837495; 43.87076142
Couthezon (Graviouse)	Nimes F	1993	BRGM/ UPVI	Ghafiri Thesis 2015	None	1?	Trenching	?				Liquefaction in Rissian terrace	Description in PhD Thesis of Ghafiri [1995]	4.88220521; 44.10044986

Table A1. (continued)

Location trench site name	Fault system	Date	Operator/ funding	Report/ thesis	Dating or stratigraphic attribution	Nb trenches	Works	Log	Boreholes	Geoph methods	Available seismic reflexion profile	EQ event(s)/ other	Published paper(s) and/data base	Trench location: [Trench number] (longitude; latitude) DDD.ddddd
La Fare (thrust) (Roustan)	Westward extension of Aix-Eguilles fault? From Terrier et al. [2008]	1994	IPSN/ GEOTER	Draft. log. and pictures	None	3	Trenching	Yes			81SE5B (in Terrier et al. [2008])	Truncated. no sediment	Coudoux. near la Fare [Baize et al, 2002]	T1: 5.15935469; 43.55705058 T2: 5.16175443; 43.55691373 T3: 5.15798180; 43.55737710
Volx-Fontamauri	MDF	1995	IPSN/ GEOTER	IPSN/GEOTER unpublished report	?	1	Trenching	Yes			Yes (IFP. total reports. CEA reprocessing)	Truncated by very recent torrential debris flows—	Grellet et al. [1995]	5.83011360; 43.87192765
Maragrate	Vinon secondary F (Vinon Thrust?) (NW–SE) (MDF)	1995	IPSN/ GEOTER	Unpublished report— Geoter cited in Thomas [2018], Thomas et al. [2020]	?/analog facies; sampling (dating?)	2	Trenching	Yes				≥1	No published document; field trip exposure during 1995 EERI int. congress [Grellet et al., 1995]; exposures presented in Thomas [2018]	T1: 5.81180567; 43.71937172 T2: 5.81162694; 43.71939388
Achenheim–Hangenbieten	URG western border F	1996	IPSN/ GEOTER (PALEOSIS CEE project)	Several IPSN un-published reports	^{14}C/UTh38- 27 ka OSL (Loess) 278–188 ka (transposed from quarry samples)	2	Trenching	Yes		HR seismic reflexion. ERT	85ST13	≥1; possibly gravita-tional	Lemeille et al. [1999b]	T1: 7.62338107; 48.57219313 T2: 7.62400631; 48.57214869 T3: 7.62418081; 48.57197847 T4: 7.61653021; 48.56456010
Riedseltz	Riedseltz– Landau fault	1996	IPSN (PALEOSIS EU project)	IPSN un-published report	No local dating. Stratigraphic correlations. Wurmian and Holocene		Outcrop cleaning and log [Geoter, 1997]	Yes		GPR. ERT [Bano et al., 2002]			Baize et al. [2002]	7.9652910; 49.00594300

Table A1. (continued)

Location trench site name	Fault system	Date	Operator/ funding	Report/ thesis	Dating or stratigraphic attribution	Nb trenches	Works	Log Boreholes	Geoph methods	Available seismic réflexion profile	EQ event(s)/ other	Published paper(s) and/data base	Trench location: [Trench number] (longitude; latitude) DDD.ddddd
Longueville/ Gourgan-con	Seine F (??) / glacitecton-ics	1997	IRSN/Univ Nancy/ P. Benoit	Master thesis	No	1	Outcrop cleaning	Yes	GPR	80RY1	Glaci tectonics interpreta-tion	Baize et al. [2007]	3.93207214; 48.55214302 4.03530251; 48.68407533
Trevaresse– Collavery	Trevaresse F	2002	IPGP/ CEREGE (ACI Lambesc)	Visit report (IRSN)	?	2	Trenching	No	ERT [Nguyen et al., 2007]	Extrapolated from 81SE5B (in Terrier et al. [2008])	No Quaternary cover truncated	Previously to the trench: [Lacassin et al., 2001, Nguyen et al., 2007]	5.35431159; 43.62016479
Reinach (Basel area)	Basel– Reinach Fault	1999	IPGS– PALEOSIS & SAFE project EC; (ETHZ). HSK (Swiss Federal Nuclear Safety In-spectorate)	PhD Ferry 2004; Paleosis research group field trip	^{14}C (Trenches ~11,500 cal. B.P.—Present) TL dating (Terraces 117-21 ky BC)	7	Trenching	Yes	ERT. HRSR	BL 24 commercial seismic line (1978) in cited literature	5	Meghraoui et al. [2001], Ferry [2004], Ferry et al. [2005]	T1: 7.61653021; 48.56456010 T2: 7.59510292; 47.51065279 T3: 7.59549090; 47.51117212 T4: 7.59451561; 47.51076315 T5: 7.59407041; 47.51031861 TA: 7.58190210; 47.48140342 T6: 7.59600806; 47.51257949 TBarsch: 7.61010447; 47.53539038
Arcizac	Lourdes fault	2003	EOST/ IPGS	PhD [Alasset, 2005]	^{14}C (Cal. 12100BP-3100 BP)	1	Trenching	Yes	GPR		1?	Alasset and Meghraoui [2005]	−0.31001539; 43.09906708
Capbis	Lourdes fault	2003	EOST/ IPGS	PhD [Alasset, 2005]	^{14}C (Cal. −22600 BP-1647 AD)	1	Trenching	Yes	GPR		1?	Alasset and Meghraoui [2005]	0.00908873; 43.09925519
Trévaresse– Ganay	Trevaresse F (main seg-ment)	2002– 2003	CEREGE/ ACI Lambesc SAFE European project	Nguyen et al. [2007]	^{14}C (historic)	2	Trenching	Yes	ERT	Extrapolated from 81SE5B (in Terrier et al. [2008])	Truncated. sealed by historic deposits	[Nguyen et al., 2007, Chardon et al., 2009] (+pers. Comm.)	T1: 5.42619848; 43.60418467 T2: 5,42722; 43.60157

(continued on next page)

Table A1. (continued)

Location trench site name	Fault system	Date	Operator/ funding	Report/ thesis	Dating or stratigraphic attribution	Nb trenches	Works	Log	Boreholes	Geoph methods	Available seismic réflexion profile	EQ event(s)/ other	Published paper(s) and/data base	Trench location: [Trench number] (longitude; latitude) DDD.ddddd
Trévaresse–Ermitage	Ermitage fault	2004/ 2006	CEREGE/ ACI Lambesc/ SAFE European project	Publications. Field report IRSN	OSL—400– 125 ky	2	Trenching	Yes		ERT	Extrapolated from 81SE5B (in Terrier et al. [2008])	≥3 max 10	[Chardon et al., 2005, 2009]; Chardon (pers. Comm); [Nguyen et al., 2007]	T1 (E): 5.41546079; 43.60172884 T2 (W): 5.41483486; 43.60183321
La Forestière	MDF	2004	CEREGE/ IRSN	Baroux PhD [Nguyen et al., 2007]. Intern reports IRSN/ CEREGE	^{14}C not processed? Roman tiles found at the trench bottom	1	Trenching	Yes	Yes	HRSR. ERT GPR	Yes (IFP. Total reports. CEA reprocessing)	No fault observed inferred from geophysics and boreholes	Siame et al. [2004] (dating. geophysics)	5.82408284; 43.83457515
Aiguilles-Rouges	Remuaz-fault	2004	EOST/ IPGS	PhD [Alasset, 2005]	Cosmogenic 10Be surface dating (post 15 ky)	2	« Mini Trenches »	No pictures		GPR		? (1905 EQ? or gravitational)	Cara et al. [2017]	6.91551306; 46.00085012
Meythet (Annecy)	Vuache Fault	2007/ 2009	IRSN	IRSN unpublished reports	Yes. OSL. ^{14}C	2		Yes		ERT. HVSR	88SVO10	No obvious surface faulting	Baize et al. [2011]	T1: 6.09507530; 45.92989931 T2: 6.09982432; 45.92523106
Sallenove (Vuache fault)	Vuache fault	2014	IRSN/U. Savoie Mt Blanc	PhD De La Taille [2015]	^{14}C (~500 cal. B.P.)	1	Trenching	Yes		ERT. GPR		No sediments too young		5.97870761; 46.00886254
Brison St Innocent (Culoz fault)	Culoz Fault	2015	IRSN/U. Savoie Mt Blanc	PhD De La Taille [2015] Master thesis [Ribot, 2015]	^{14}C—OSL (45–48 ky)	1	Outcrop cleaning	Yes		ERT		No single event. But pluri-metric deformation	Jomard et al. [2017]	5.89464919; 45.72656808

Table A1. (continued)

Location trench site name	Fault system	Date	Operator/ funding	Report/ thesis	Dating or stratigraphic attribution	Nb trenches	Works	Log	Boreholes	Geoph methods	Available seismic réflexion profile	EQ event(s)/ other	Published paper(s) and/data base	Trench location: [Trench number] (longitude; latitude) DDD.ddddd
Maragrate	Vinon secondary F (MDF)	2016	CEREGE/ CEA	PhD [Thomas, 2018]	^{14}C. OSL	1	Trenching	Yes		LiDAR. ERT		≥1?	Thomas [2018], Thomas et al. [2020]	T3: 5.81126570; 43.71946812
Riedseltz	Riedseltz– Landau fault	<2016	Shipton et al. [2017]	Shipton et al. [2017]	No local dating. Stratigraphic correlations. Wurmian and Holocene			Yes		GPR. ERT [Bano et al., 2002]			Shipton et al. [2017]	
Ettligen (Germany)	Eastern central Rhine Graben Boundary fault	2019	RWTH/ IRSN/IGV/ USD.KIT. CGS	EGU abstract	14C (in progress)	6	Trenching	Yes		ERT.GPR		≥2	Reicherter et al. [2020] (work in progress)	8.38862987; 48.91329790
La Rouvière fault	Cevennes fault system	2019–2020	U. Montpellier/IRSN/ CEREGE/U Nice etc ???	Raw and draft reports (Ritz and coll.); Baize *et al.* (soc Ardeche)	^{14}C. OSL.	>10	Trenching	Yes		???. HVSR	???	>1?	Ritz et al. [2020, 2021b]	TD (LRT1); 4.65616685; 44.52360212 (more than 10 trenches). Work in progress
Osthofen (Germany)	West border fault	2003	EUCOR-URGENT project and the EU project of Environmental Tectonics (ENTEC). (GRS) mbH. ISES, DAAD	Peters PhD thesis, [Peters et al., 2005]	TL and ^{14}C	3	Trenching, coring	Yes	Yes	High res. seismic reflection, ERT, GPR	Not precisely indicated	One single EQ (mw 6.5) or creep deformation (0.5 m) between 19 and 8 ka, but possible interplay between tectonic activity and fluvial and erosional processes	Peters et al. [2005]	T1: 8.31607; 49.721874 T2: 8.315363; 49.721787 T3 : 8.315072; 49.720951

References

Ahorner, L. (1983). Historical seismicity and present-day microearthquake activity of the Rhenish Massif, central Europe. In Fuchs, K., von Gehlen, K., Mälzer, H., Murawski, H., and Semmel, A., editors, *Plateau Uplift*, pages 198–221. Springer, Berlin, Germany.

Alasset, P.-J. (2005). *Sismotectonique et identification des sources sismiques en domaine à déformation lente : Cas des Pyrénées Occidentales et des Alpes du Nord (France). Le tsunami créé par le séisme de Zemmouri ($M_w = 6.9$, Algérie) du 21 Mai 2003.* PhD thesis.

Alasset, P.-J. and Meghraoui, M. (2005). Active faulting in the western Pyrénées (France): paleoseismic evidence for late Holocene ruptures. *Tectonophysics*, 409, 39–54.

Anikiev, D., Cacace, M., Bott, J., Gomez Dacal, M. L., and Scheck-Wenderoth, M. (2020). Influence of lithosphere rheology on seismicity in an intracontinental rift: the case of the Rhine Graben. *Front. Earth Sci.*, 8, article no. 592561.

Asensio, E., Khazaradze, G., Echeverria, A., King, R. W., and Vilajosana, I. (2012). GPS studies of active deformation in the Pyrenees. *Geophys. J. Int.*, 190, 913–921.

Baize, S., Coulon, M., Hibsch, C., Cushing, M., Lemeille, F., and Hamard, E. (2007). Non-tectonic deformations of Pleistocene sediments in the eastern Paris basin, France. *Bull. Soc. Geol. Fr.*, 178, 367–381.

Baize, S., Cushing, E. M., Lemeille, F., Granier, T., Grellet, B., Combes, P., and Hibsch, C. (2002). Inventaire des indices de rupture affectant le Quaternaire en relation avec les grandes structures connues, en France métropolitaine et dans les régions limitrophes. *Mém. Soc. Géol. Fr. Mémoire H.S.*, (175).

Baize, S., Cushing, M., Lemeille, F., Gelis, C., Texier, D., Nicoud, G., and Schwenninger, J.-L. (2011). Contribution to the seismic hazard assessment of a slow active fault, the Vuache fault in the southern Molasse basin (France). *Bull. Soc. Geol. Fr.*, 182, 347–365.

Baize, S., Nurminen, F., Sarmiento, A., Dawson, T., Takao, M., Scotti, O., Azuma, T., Boncio, P., Champenois, J., Cinti, F. R., Civico, R., Costa, C., Guerrieri, L., Marti, E., McCalpin, J., Okumura, K., and Villamor, P. (2020). A worldwide and unified database of surface ruptures (SURE) for fault displacement hazard analyses. *Seismol. Res. Lett.*, 91, 499–520.

Bano, M., Edel, J.-B., Herquel, G., and EPGS class 2001–2002 (2002). Geophysical investigation of a recent shallow fault. *Lead. Edge*, 21, 648–650.

Baroux, E. (2000). *Tectonique active en région à sismicité modérée : le cas de la Provence (France): apport d'une approche pluridisciplinaire.* PhD thesis, Université Paris 11.

Baroux, E., Béthoux, N., and Bellier, O. (2001). Analyses of the stress field in southeastern France from earthquake focal mechanisms. *Geophys. J. Int.*, 145, 336–348.

Baroux, E., Pino, N. A., Valensise, G., Scotti, O., and Cushing, M. E. (2003). Source parameters of the 11 June 1909, Lambesc (Provence, southeastern France) earthquake: a reappraisal based on macroseismic, seismological, and geodetic observations. *J. Geophys. Res.*, 108(B9), article no. 2454.

Barth, A., Ritter, J. R. R., and Wenzel, F. (2015). Spatial variations of earthquake occurrence and coseismic deformation in the Upper Rhine Graben, central Europe. *Tectonophysics*, 651–652, 172–185.

Bartz, J. (1974). Die Mächtigkeit des Quartärs im Oberrheingraben. In Illies, J. H. and Fuchs, K., editors, *Approaches to Taphrogenesis*, Inter-union Commission Geodynamics Scientific Report, 8, pages 78–87.

BDFA, I. (2020). Database of potentially active faults (BDFA) for Metropolitan France. https://bdfa.irsn.fr/.

Beck, C., Manalt, F., Chapron, E., Van Rensbergen, P., and De Batist, M. (1996). Enhanced seismicity in the early post-glacial period: evidence from the post-Würm sediments of Lake Annecy, northwestern Alps. *J. Geodyn.*, 22, 155–171.

Bellier, O. (2014). Tremblements de terre et aléa sismique, l'apport de la tectonique active et de la paléosismologie. *Géologues — Géologie Fr. Quoi Neuf*, 180, 93–97.

Bertrand, G., Horstmann, M., Hermann, O., and Behrmann, J. H. (2005). Retrodeformation of the southern Upper Rhine Graben: new insights on continental oblique rifting. *Quat. Sci. Rev.*, 24, 345–352.

Bestani, L., Espurt, N., Lamarche, J., Bellier, O., and Hollender, F. (2016). Reconstruction of the provence chain evolution, southeastern France. *Tectonics*, 35, 1506–1525.

Bestani, L., Espurt, N., Lamarche, J., Floquet, M., Philip, J., Bellier, O., and Hollender, F. (2015). Structural style and evolution of the Pyrenean-Provence thrust belt, SE France. *Bull. Soc. Geol. Fr.*, 186, 223–241.

Billant, J., Bellier, O., Godard, V., and Hippolyte, J.-C. (2016). Constraining recent fault offsets with statistical and geometrical methods: example from the Jasneuf Fault (Western Alps, France). *Tectonophysics*, 693, 1–21.

Billant, J., Hippolyte, J.-C., and Bellier, O. (2015). Tectonic and geomorphic analysis of the Belledonne border fault and its extensions, Western Alps. *Tectonophysics*, 659, 31–52.

Bonjer, K. P., Gelbke, C., Gilg, B., Rouland, D., Mayer-Rosa, D., and Massinon, B. (1984). Seismicity and dynamics of the Upper Rhine graben. *J. Geophys.—Z. Geophys.*, 55, 1–12.

Buraczynski, J. and Butrym, J. (1984). La datation des loess du profil d'Achenheim (Alsace) à l'aide de la méthode de thermoluminescence. *Bull. de l'Ass. française pour l'Étude du Quaternaire*, 21(4), 201–209.

Burkhard, M. (1990). Aspects of the large-scale Miocene deformation in the most external part of the Swiss Alps (Subalpine Molasse to Jura fold belt). *Eclogae Geol. Helv.*, 83, 559–583.

Calais, E., Camelbeeck, T., Stein, S., Liu, M., and Craig, T. J. (2016). A new paradigm for large earthquakes in stable continental plate interiors. *Geophys. Res. Lett.*, 43, 10621–10637.

Calvet, M. (1996). Morphogenèse d'une montagne méditérranéenne les Pyrénées orientales. In *Documents du BRGM géologie régionale et générale 255*. BRGM, Orléans, France.

Camelbeeck, T. and Meghraoui, M. (1998). Geological and geophysical evidence for large palaeo-earthquakes with surface faulting in the Roer Graben (northwest Europe). *Geophys. J. Int.*, 132, 347–362.

Capella, W., Bellier, O., Hippolyte, J.-C., Cushing, E. M., Delanghe-Sabatier, D., Hermitte, D., and Parisot, J.-C. (2014). Interaction canyon messinien et faille de Nîmes dans le secteur du bassin de Pujaut: apport quant à l'évaluation des aléas locaux/régionaux. In *Presented at the 24eme Réunion des Sciences de la Terre, Pau, France*.

Cara, M., Cansi, Y., Schlupp, A., Arroucau, P., Béthoux, N., Beucler, E., Bruno, S., Calvet, M., Chevrot, S., Deboissy, A., Delouis, B., Denieul, M., Deschamps, A., Doubre, C., Fréchet, J., Godey, S., Golle, O., Grunberg, M., Guilbert, J., Haugmard, M., Jenatton, L., Lambotte, S., Leobal, D., Maron, C., Mendel, V., Merrer, S., Macquet, M., Mignan, A., Mocquet, A., Nicolas, M., Perrot, J., Potin, B., Sanchez, O., Santoire, J.-P., Sèbe, O., Sylvander, M., Thouvenot, F., Van Der Woerd, J., and Van Der Woerd, K. (2015). SI-Hex: a new catalogue of instrumental seismicity for metropolitan France. *Bull. Soc. Geol. Fr.*, 186, 3–19.

Cara, M., Van der Woerd, J., Alasset, P.-J., Benjumea, J., and Mériaux, A.-S. (2017). The 1905 Chamonix earthquakes: active tectonics in the Mont Blanc and Aiguilles Rouges massifs. *Swiss J. Geosci.*, 110, 631–651.

Carbon, D., Combes, P., Cushing, M., and Granier, T. (1993). Enregistrement d'un paléoséisme dans des sédiments du Pléistocène supérieur dans la vallée du Rhône: quantification de la déformation. *Géol. Alp.*, 69, 33–48.

Carbon, D., Combes, P., Cushing, M., Granier, T., and Grellet, B. (1995). Post middle-Pleistocene tectonic surface ruptures in the Aquitaine Basin [Rupture de surface post-Pleistocene moyen dans le Bassin aquitain]. *C. R. Acad. Sci. Ser. II Sci. Terre Planetes*, 320, 311–317.

Champion, C., Choukroune, P., and Clauzon, G. (2000). Post Miocene deformation of Western Provence [La deformation post-Miocene en Provence occidentale]. *Geodin. Acta*, 13, 67–85.

Chapron, E., Van Rensbergen, P., Beck, C., De Batist, M., and Paillet, A. (1996). Lacustrine sedimentary records of brutal events in Lake Le Bourget (Northwestern Alps-Southern Jura). *Quaternaire*, 7, 155–168.

Chardon, D. and Bellier, O. (2003). Geological boundary conditions of the 1909 Lambesc (Provence, France) earthquake: structure and evolution of the Trévaresse ridge anticline. *Bull. Soc. Geol. Fr.*, 174, 497–510.

Chardon, D., Hermitte, D., Nguyen, F., and Bellier, O. (2005). First paleoseismological constraints on the strongest earthquake in France (Provence) in the twentieth century. *Geology*, 33, 901–904.

Chardon, D., Hermitte, D., Parisot, J.-C., Dussouillez, P., and Nguyen, F. (2009). Geology, tectonic geomorphology and seismic hazard of the Trévaresse fault, the source of the 1909 Lambesc earthquake.

In *International Conference Provence' 2009 — Aix-En-Provence (France) — July, 6–8, 2009.*

Chevrot, S., Sylvander, M., and Delouis, B. (2011). A preliminary catalog of moment tensors for the Pyrenees. *Tectonophysics*, 510, 239–251.

Clauzon, G., Aguilar, J.-P., and Michaux, J. (1989). Investigation of the time-sedimentation relation thanks the French Mediterranean Neogene [Relation temps-sedimentation dans le Neogene mediterraneen francais]. *Bull. Soc. Geol. Fr.*, 5, 361–372.

Clauzon, G., Fleury, J., Bellier, O., Molliex, S., Mocochain, L., and Aguilar, J.-P. (2011). Morphostructural evolution of the Luberon since the Miocene (SE France). *Bull. Soc. Geol. Fr.*, 182, 95–110.

Clauzon, G., Fleury, J., and Schlupp, A. (2004). Evolution géodynamique du Bas-Rhône (section Orange/Beaucaire) depuis 6 Ma. Apport Méthode Niveaux Repères Messin. Ainsi Que Terrasses Quat. Intégrés À Outil SIG Rapp. CEA-CEREGE.

Combes, P. (1984). *La tectonique récente de la Provence occidentale microtectonique, caractéristiques dynamiques et cinématiques : méthodologie de zonation tectonique et relations avec la séismicité.* PhD thesis, Université de Strasbourg.

Combes, P. and Carbon, D. (1997). Néotectonique et sismicité du Gard Rhodanien. In *Etude Du Gard Rhodanien : Actes Des Journées Scientifiques CNRS/ANDRA, Bagnols-sur-Ceze, 20 et 21 Octobre 1997*, pages 94–114. EDP Sciences.

Combes, P., Carbon, D., Cushing, M., Granier, T., and Vaskou, P. (1993). Identification of an Upper Pleistocene palaeoearthquake in the Rhone Valley: implications for the understanding of seismicity in France [Mise en evidence d'un paleoseisme pleistocene superieur dans la vallee du Rhone: implications sur les connaissances de la sismicite en France]. *C. R. Acad. Sci. Ser. II*, 317, 689–696.

Cornou, C., Ampuero, J.-P., Aubert, C., Audin, L., Baize, S., Billant, J., Brenguier, F., Causse, M., Chlieh, M., Combey, A., Michele, M., de, Delouis, B., Deschamps, A., Ferry, M., Foumelis, M., Froment, B., Gélis, C., Grandin, R., Grasso, J.-R., Hannouz, E., Hok, S., Jung, A., Jolivet, R., Langlais, M., Langlaude, P., Larroque, C., Leloup, P. H., Manchuel, K., Marconato, L., Maron, C., Mathot, E., Maufroy, E., Mercerat, D., Metois, M., Nayman, E., Pondaven, I., Provost, L., Régnier, J., Ritz, J.-F., Rivet, D., Schlupp, A., Sladen, A., Voisin, C.,

Walpersdorf, A., Wolynieck, D., Allemand, P., Beck, E., Bertrand, E., Bertrand, V., Briole, P., Brunel, D., Cavalié, O., Chèze, J., Courboulex, F., Douste-Bacque, I., Dretzen, R., Giampietro, T., Godano, M., Grandjean, P., Grunberg, M., Guerin, G., Guillot, S., Haber, E. E., Hernandez, A., Jomard, H., Lasserre, C., Liang, C., Lior, I., Martin, X., Mata, D., Menager, M., Mercier, A., Mordret, A., Oral, E., Paul, A., Peix, F., Pequegnat, C., Pernoud, M., Satriano, C., Sassi, R., Schaming, M., Sellier, V., Sira, C., Socquet, A., Sue, C., Trilla, A., Vallée, M., Ende, M. v. d., Vernant, P., Vial, B., and Weng, H. (2021). Rapid response to the M_w 4.9 earthquake of November 11, 2019 in Le Teil, Lower Rhône Valley, France. *C. R. Géosci.*, 353(S1), 441–463.

Courboulex, F., Larroque, C., Deschamps, A., Kohrssansorny, C., Gélis, C., Got, J. L., Charreau, J., Stéphan, J. F., Béthoux, N., Virieux, J., Brunel, D., Maron, C., Duval, A. M., Perez, J.-L., and Mondielli, P. (2007). Seismic hazard on the French Riviera: observations, interpretations and simulations. *Geophys. J. Int.*, 170, 387–400.

Cushing, E. M., Bellier, O., Nechtschein, S., Sébrier, M., Lomax, A., Volant, P. H., Dervin, P., Guignard, P., and Bove, L. (2008). A multidisciplinary study of a slow-slipping fault for seismic hazard assessment: the example of the Middle Durance Fault (SE France). *Geophys. J. Int.*, 172, 1163–1178.

Cushing, M., Baize, S., Guignard, P., Bellier, O., Siame, L., Nguyen, F., and Garambois, S. (2005). Estimation de l'aléa simogénique d'une faille active du Sud-Est de la France – Paléosismicité de la faille de la Moyenne Durance dans la région de Manosque. IRSN report DEI/SARG/2005-014.

De La Taille, C. (2015). *Évaluation de l'activité tectonique quaternaire des failles du Jura Méridional (France).* PhD thesis, Université Grenoble Alpes.

de Vicente, G., Cloetingh, S., Muñoz Martín, A., Olaiz, A., Stich, D., Vegas, R., Galindo-Zaldívar, J., and Fernández-Lozano, J. (2008). Inversion of moment tensor focal mechanisms for active stresses around the microcontinent Iberia: tectonic implications. *Tectonics*, 27, article no. TC1009.

Doubre, C., Meghraoui, M., Masson, F., Lambotte, S., Jund, H., Bès de Berc, M., and Grunberg, M. (2021). Seismotectonics in Northeastern France and neighboring regions. *C. R. Géosci.*, 353(S1), 153–185.

Dutour, A., Philip, H., Jaurand, E., and Combes, P.

(2002). Evidence of reverse faulting and coseismic surface ruptures in Würm colluvial deposits from the Mt Ventoux northern slope (Western Provence, France) [Mise en évidence de déformations en faille inverse avec ruptures de surface cosismiques dans des dépôts colluviaux würmiens du versant nord du mont Ventoux (Provence occidentale, France)]. *C. R. Geosci.*, 334, 849–856.

Fäh, D., Gisler, M., Jaggi, B., Kästli, P., Lutz, T., Masciadri, V., Matt, C., Mayer-Rosa, D., Rippmann, D., Schwarz-Zanetti, G., Tauber, J., and Wenk, T. (2009). The 1356 Basel earthquake: an interdisciplinary revision. *Geophys. J. Int.*, 178, 351–374.

Ferry, M., Meghraoui, M., Delouis, B., and Giardini, D. (2005). Evidence for Holocene palaeoseismicity along the Basel–Reinach active normal fault (Switzerland): a seismic source for the 1356 earthquake in the Upper Rhine graben. *Geophys. J. Int.*, 160, 554–572.

García-Moreno, D., Gupta, S., Collier, J. S., Oggioni, F., Vanneste, K., Trentesaux, A., Verbeeck, K., Versteeg, W., Jomard, H., Camelbeeck, T., and De Batist, M. (2019). Middle-Late Pleistocene landscape evolution of the Dover Strait inferred from buried and submerged erosional landforms. *Quat. Sci. Rev.*, 203, 209–232.

Ghafiri, A. (1995). Paléosismicité de failles actives en contexte de sismicité modérée : application à l'évaluation de l'aléa sis-mique dans le Sud-Est de la France. Orsay, Paris Sud.

Giamboni, M., Wetzel, A., Nivière, B., and Schumacher, M. (2004). Plio-Pleistocene folding in the southern Rhinegraben recorded by the evolution of the drainage network (Sundgau area; northwestern Switzerland and France). *Eclogae Geol. Helv.*, 97, 17–31.

Gilli, É. (2005). Review on the use of natural cave speleothems as palaeoseismic or neotectonics indicators. *C. R. Geosci.*, 337, 1208–1215.

Godard, V., Hippolyte, J.-C., Cushing, E., Espurt, N., Fleury, J., Bellier, O., and Ollivier, V. (2020). Hillslope denudation and morphologic response to a rock uplift gradient. *Earth Surf. Dyn.*, 8, 221–243.

Godard, V., Ollivier, V., Bellier, O., Miramont, C., Shabanian, E., Fleury, J., Benedetti, L., and Guillou, V. (2016). Weathering-limited hillslope evolution in carbonate landscapes. *Earth Planet. Sci. Lett.*, 446, 10–20.

Grellet, B. and Combes, P. (1995). Etude tectonique du chevauchement de Vinon – Analyse de la déformation récente en termes de paléosismicité. Rapport Geoter cited in Thomas et al. (2020).

Grellet, B., Combes, P., Granier, T., and Cushing, E. M. (1995). The Durance fault system. In *A field trip for the Fifth International Conference on Seismic Zonation. Presented at the 5th International Conference on Seismic Zonation, A.F.P.S.-E.E.R.I. (Ouest Editions); October 17–19 1995, Nice, France.*

Grellet, B., Combes, P., Granier, T., and Philip, H. (1993). Sismotectonique de la France métropolitaine dans son cadre géologique et géophysique, avec atlas de 23 cartes au 1:4000 000 et une carte au 1:1000 000. Mémoire de la Société Géologique de France.

Griffin, M. J., Bragagnolo, L. J., and Yanev, P. I. (1991). The December 7, 1988, Armenia earthquake: Effects on selected power, industrial, and commercial facilities. Report No. EPRI-NP–7359-M, ref 23007599 for Electric Power Research Inst., Palo Alto, CA (United States). IAEA INIS Volume 23, Issue 3. https://inis.iaea.org/search/search.aspx?orig_q=RN:23007599 last accessed December 11, 2021.

Guyonnet-Benaize, C., Lamarche, J., Hollender, F., Viseur, S., Münch, P., and Borgomano, J. (2015). Three-dimensional structural modeling of an active fault zone based on complex outcrop and subsurface data: the Middle Durance Fault Zone inherited from polyphase Meso-Cenozoic tectonics (southeastern France). *Tectonics*, 34, 265–289.

Hippolyte, J.-C., Bourlès, D., Léanni, L., Braucher, R., Chauvet, F., and Lebatard, A. E. (2012). ^{10}Be ages reveal >12 ka of gravitational movement in a major sackung of the Western Alps (France). *Geomorphology*, 171–172, 139–153.

Hippolyte, J.-C. and Dumont, T. (2000). Identification of quaternary thrusts, folds and faults in a low seismicity area: examples in the Southern Alps (France). *Terra Nova*, 12, 156–162.

Hürtgen, J. (2017). The First Paleoseismic Database of Germany and Adjacent Regions PalSeisDB v1.0. RWTH Aachen University, Aachen.

Hürtgen, J., Reicherter, K., Spies, T., Geisler, C., and Schlittenhardt, J. (2020). The Paleoseismic Database of Germany and Adjacent Regions PalSeisDB. V. 1.0. GFZ Data Services.

IAEA TECDOC No. 1767 (2015). *The Contribution of Palaeoseismology to Seismic Hazard Assessment*

in Site Evaluation for Nuclear Installations. TEC-DOC Series. International Atomic Energy Agency, Vienna, Austria.

Jomard, H., Cushing, E. M., Palumbo, L., Baize, S., David, C., and Chartier, T. (2017). Transposing an active fault database into a seismic hazard fault model for nuclear facilities—Part 1: Building a database of potentially active faults (BDFA) for metropolitan France. *Nat. Hazards Earth Syst. Sci.*, 17, 1573–1584.

Kaub, C. (2019). *Déformation active intraplaque : étude pluridisciplinaire terre-mer du risque sismique en Vendée, à partir du séisme du Marais Breton de 1799*. PhD thesis, Université de Bretagne occidentale — Brest.

Kelsey, H. M., Sherrod, B. L., Nelson, A. R., and Brocher, T. M. (2008). Earthquakes generated from bedding plane-parallel reverse faults above an active wedge thrust, Seattle fault zone. *Bull. Geol. Soc. Am.*, 120, 1581–1597.

Kremer, K., Gassner-Stamm, G., Grolimund, R., Wirth, S. B., Strasser, M., and Fäh, D. (2020). A database of potential paleoseismic evidence in Switzerland. *J. Seismol.*, 24, 247–262.

Lacan, P. and Ortuño, M. (2012). Active tectonics of the Pyrenees: a review. *J. Iber. Geol.*, 38, 9–30.

Lacassin, R., Tapponnier, P., Meyer, B., and Armijo, R. (2001). Was the Trévaresse thrust the source of the 1909 Lambesc (Provence, France) earthquake? Historical and geomorphic evidence. *C. R. Acad. Sci.—Ser. IIA—Earth Planet. Sci.*, 333, 571–581.

Lambert, J., Winter, T., Dewez, T. J. B., and Sabourault, P. (2005). New hypotheses on the maximum damage area of the 1356 Basel earthquake (Switzerland). *Quat. Sci. Rev.*, 24, 381–399.

Larroque, C., Baize, S., Albaric, J., Jomard, H., Trévisan, J., Godano, M., Cushing, M., Deschamps, A., Sue, C., Delouis, B., Potin, B., Courboulex, F., Régnier, M., and Rivet, D. (2021). Seismotectonics of southeast France: From the Jura mountains to Corsica. *C. R. Géosci.*, 353(S1), 105–151.

Laubscher, H. (1992). Jura kinematics and the Molasse Basin. *Eclogae Geol. Helv.*, 85, 653–675.

Laubscher, H. (2008). 100 years Jura décollement hypothesis: How it affects Steinmann's (1892) "Schwarzwaldlinie.". *Int. J. Earth Sci.*, 97, 1231–1245.

Le Pichon, X., Rangin, C., Hamon, Y., Loget, N., Lin, J. Y., Andreani, L., and Flotte, N. (2010). Geodynamics of the france southeast basin. *Bull. Soc. Geol. Fr.*, 181, 477–501.

Lemeille, F., Cushing, M., Carbon, D., Grellet, B., Bitterli, T., Flehoc, C., and Innocent, C. (1999a). Coseismic ruptures and deformations recorded by speleothems in the epicentral zone of the basel earthquake. *Geodin. Acta*, 12, 179–191.

Lemeille, F., Cushing, M. E., Cotton, F., Grellet, B., Ménillet, F., Audru, J.-C., Renardy, F., and Fléhoc, C. (1999b). Evidence for middle to late Pleistocene faulting within the northern Upper Rhine Graben (Alsace Plain, France) [Traces d'activité pléistocène de failles dans le Nord du fosse du Rhin supérieur (plaine d'alsace, France)]. *C. R. Acad. Sci.—Ser. IIa Sci. Terre Planetes*, 328, 839–846.

Leonard, M. (2010). Earthquake fault scaling: Self-consistent relating of rupture length, width, average displacement, and moment release. *Bull. Seismol. Soc. Am.*, 100, 1971–1988.

Manchuel, K., Traversa, P., Baumont, D., Cara, M., Nayman, E., and Durouchoux, C. (2018). The French seismic CATalogue (FCAT-17). *Bull. Earthq. Eng.*, 16, 2227–2251.

Mathey, M., Sue, C., Pagani, C., Baize, S., Walpersdorf, A., Bodin, T., Husson, L., Hannouz, E., and Potin, B. (2021). Present-day geodynamics of the Western Alps: new insights from earthquake mechanisms. *Solid Earth*, 12, 1661–1681.

Mattauer, M. (2002). Commentaire sur l'article : "Mouvement post-messinien sur la faille de Nîmes …" par A. Schlupp et al. *Bull. Soc. Geol. Fr.*, 173, 595.

Mazzotti, S., Jomard, H., and Masson, F. (2020). Processes and deformation rates generating seismicity in metropolitan France and conterminous Western Europe. *BSGF—Earth Sci. Bull.*, 191, article no. 19.

McCalpin, J. P. (2009). *Paleoseismology*, volume 95 of *International Series*. Academic Press, 2nd edition.

Meghraoui, M., Delouis, B., Ferry, M., Giardini, D., Huggenberger, P., Spottke, I., and Granet, M. (2001). Active normal faulting in the upper Rhine graben and paleoseismic identification of the 1356 basel earthquake. *Science*, 293, 2070–2073.

Meyer, B., Lacassin, R., Brulhet, J., and Mouroux, B. (1994). The Basel 1356 earthquake: which fault produced it? *Terra Nova*, 6, 54–63.

Molliex, S., Fabbri, O., Bichet, V., and Madritsch, H. (2011). Possible quaternary growth of a hidden anticline at the front of the Jura fold-and-thrust

belt: geomorphological constraints from the Forêt de Chaux area, France. *Bull. Soc. Geol. Fr.*, 182, 337–346.

Monninger, R. (1985). *Neotektonische Bewegungsmechanismen im mittleren Oberrheingraben.* PhD thesis, Universität Karlsruhe.

NEOPAL (2009). Base de données nationale des déformations récentes et des paléoséismes. National database of recent deformations and paleoearthquakes. Now on the web site GEORISQUES (https://www.georisques.gouv.fr/risques/seismes/donnees#/).

Neopal report (2008). Base de données Neopal — Travaux des experts, avril à décembre 2008. Rapport final BRGMRP-56981-FR.

Nguyen, F., Garambois, S., Chardon, D., Hermitte, D., Bellier, O., and Jongmans, D. (2007). Subsurface electrical imaging of anisotropic formations affected by a slow active reverse fault, Provence, France. *J. Appl. Geophys.*, 62, 338–353.

Nivière, B., Bruestle, A., Bertrand, G., Carretier, S., Behrmann, J., and Gourry, J.-C. (2008). Active tectonics of the southeastern Upper Rhine Graben, Freiburg area (Germany). *Quat. Sci. Rev.*, 27, 541–555.

Nivière, B. and Winter, T. (2000). Pleistocene northwards fold propagation of the Jura within the southern Upper Rhine graben: seismotectonic implications. *Glob. Planet. Change*, 27, 263–288.

Nocquet, J.-M. (2002). *Mesure de la déformation crustale en Europe occidentale par géodésie spatiale.* PhD thesis, http://www.theses.fr/2002NICE5738.

Nocquet, J.-M. (2012). Present-day kinematics of the Mediterranean: a comprehensive overview of GPS results. *Tectonophysics*, 579, 220–242.

Nurminen, F., Boncio, P., Visini, F., Pace, B., Valentini, A., Baize, S., and Scotti, O. (2020). Probability of occurrence and displacement regression of distributed surface rupturing for reverse earthquakes. *Front. Earth Sci.*, 8. https://doi.org/10.3389/feart.2020.581605.

Pascual, G. (1978). Présence d'une faille à rejeu quaternaire au cellier des Princes. Courthézon (Vaucluse). *Géol. Méditerranéenne V*, 325–326.

Pascual, G. (1979). *Contribution à la connaissance du Plio-Quaternaire de la rive gauche de la moyenne vallée du Rhône (stratigraphie et tectonique).* PhD thesis, Faculté des sciences de Marseille.

Peters, G., Buchmann, T. J., Connolly, P., van Balen, R. T., Wenzel, F., and Cloetingh, S. A. P. L. (2005). Interplay between tectonic, fluvial and erosional processes along the Western Border Fault of the northern Upper Rhine Graben, Germany. *Tectonophysics*, 406, 39–66.

Peulvast, J.-P., Baroux, E., Sébrier, M., and Bellier, O. (1999). Le problème de l'activité des failles de Nîmes, de Salon-Cavaillon et de la moyenne Durance (SE de la France) : apports de la géomorphologie structurale/The problem of tectonic activity along the Nîmes, Salon-Cavaillon and moyenne Durance fault zones: evidence from structural geomorphology. *Géomorphol. Relief Process. Environ.*, 4, 327–358.

Philippe, Y. (1995). *Rampes latérales et zones de transfert dans les chaînes plissées : géométrie, condition de formation et pièges structuraux associés.* PhD thesis, Université de Savoie.

Plenefisch, T. and Bonjer, K.-P. (1997). The stress field in the Rhine Graben area inferred from earthquake focal mechanisms and estimation of frictional parameters. *Tectonophysics*, 275, 71–97.

Reicherter, K., Baize, S., Hürtgen, J., Cinti, F., Rockwell, T. K., Jomard, H., Seitz, G., and Ritter, J. (2020). Paleoseismological trenching of the eastern Rhine Graben Boundary Fault: the Ettlingen segment. In *EGU General Assembly Conference Abstracts EGU2020-6187.* On-Line.

Rigo, A., Vernant, P., Feigl, K. L., Goula, X., Khazaradze, G., Talaya, J., Morel, L., Nicolas, J., Baize, S., Chéry, J., and Sylvander, M. (2015). Present-day deformation of the pyrenees revealed by GPS surveying and earthquake focal mechanisms until 2011. *Geophys. J. Int.*, 201, 947–964.

Ritz, J.-F., Baize, S., Audin, L., Authemayou, C., Kaub, C., Lacan, P., Leclerc, F., Manchuel, K., Mugnier, J. L., Ortuño, M., Rizza, M., and Vassallo, R. (2021a). Perspectives in studying active faults in metropolitan France. *C. R. Géosci.*, 353(S1), 381–412.

Ritz, J.-F., Baize, S., Ferry, M., et al. (2020). Surface rupture and shallow fault reactivation during the 2019 Mw 4.9 Le Teil earthquake, France. *Commun. Earth Environ.*, 1, article no. 10.

Ritz, J.-F., Ferry, M., Hannouz, E., Riesner, M., Bollinger, L., Larroque, C., Audin, L., Manchuel, K., Rizza, M., Jomard, H., Sue, C., Arroucau, P., and Billant, J. (2021b). Analyzing the paleoseismic history of the La Rouvière fault, unex-

pected source of the 11-11-2019, M_w4.9 Le Teil surface rupturing earthquake (Cévennes fault system, France). In *EGU General Assembly Conference Abstracts EGU21-13044*. On-Line.

Rockwell, T. K., Ragona, D. E., Meigs, A. J., Owen, L. A., Costa, C. H., and Ahumada, E. A. (2014). Inferring a thrust-related earthquake history from secondary faulting: a long rupture record of La Laja fault, San Juan, Argentina. *Bull. Seismol. Soc. Am.*, 104, 269–284.

Roure, F., Brun, J.-P, Colletta, B., and Van Den Driessche, J. (1992). Geometry and kinematics of extensional structures in the alpine foreland basin of southeastern France. *J. Struct. Geol.*, 14, 503–519.

Roure, F. and Colletta, B. (1996). Cenozoic inversion structures in the foreland of the Pyrenees and Alps. In Ziegler, P. A. and Horvath, F., editors, *Peri-Tethys Memoir 2: Structure and Prospects of Alpine Basins and Forelands*, volume 170 of *Mém. Mus. Natn. Hisr. Nat.*, pages 173–209. Paris.

Schlupp, A., Clauzon, G., and Avouac, J.-P. (2001). Post Messinian movement along the Nîmes fault: implications for the seismotectonics of Provence (France) [Mouvement post-messinien sur la faille de Nîmes: Implications pour la sismotectonique de la Provence]. *Bull. Soc. Geol. Fr.*, 172, 697–711.

Schlupp, A., Clauzon, G., and Avouac, J. P. (2002). Réponse au commentaire sur l'article "Mouvement post-messinien sur la faille de Nîmes : implications pour la sismotectonique de la Provence". *Bull. Soc. Geol. Fr.*, 173, 592–594.

Sébrier, M., Ghafiri, A., and Bles, J.-L. (1997). Paleoseismicity in France: fault trench studies in a region of moderate seismicity. *J. Geodyn.*, 24, 207–217.

Séranne, M. (2002). Commentaire sur l'article : mouvement post-messinien sur la faille de Nîmes par Schlupp et al., 2001. *Bull. Soc. Geol. Fr.*, 173, 589–591.

Shipton, Z. K., Meghraoui, M., and Monro, L. (2017). Seismic slip on the west flank of the upper rhine graben (france-germany): evidence from tectonic morphology and cataclastic deformation bands. *Geol. Soc. Special Publ.*, 432, 147–161.

Siame, L., Bellier, O., Braucher, R., Sébrier, M., Cushing, M., Bourlès, D., Hamelin, B., Baroux, E., de Voogd, B., Raisbeck, G., and Yiou, F. (2004). Local erosion rates versus active tectonics: cosmic ray exposure modelling in Provence (south-east France). *Earth Planet. Sci. Lett.*, 220, 345–364.

Siame, L. L., Sébrier, M., Bellier, O., Bourlès, D., Costa, C., Ahumada, E. A., Gardini, C. E., and Cisneros, H. (2015). Active basement uplift of Sierra Pie de Palo (Northwestern Argentina): rates and inception from10 Be cosmogenic nuclide concentrations. *Tectonics*, 34, 1129–1153.

Souriau, A., Rigo, A., Sylvander, M., Benahmed, S., and Grimaud, F. (2014). Seismicity in central-western Pyrenees (France): a consequence of the subsidence of dense exhumed bodies. *Tectonophysics*, 621, 123–131.

Stich, D., Batlló, J., Macià, R., Teves-Costa, P., and Morales, J. (2005). Moment tensor inversion with single-component historical seismograms: the 1909 Benavente (Portugal) and Lambesc (France) earthquakes. *Geophys. J. Int.*, 162, 850–858.

Sylvander, M., Rigo, A., Sénéchal, G., Battaglia, J., Benahmed, S., Calvet, M., Chevrot, S., Douchain, J.-M., Grimaud, F., Letort, J., and Pauchet, H. (2021). Seismicity patterns in southwestern France. *C. R. Geosci.*, 353, 79–104.

Tapponnier, P., Meyer, B., Avouac, J. P., Peltzer, G., Gaudemer, Y., Shunmin, G., Hongfa, X., Kelun, Y., Zhitai, C., Shuahua, C., and Huagang, D. (1990). Active thrusting and folding in the Qilian Shan, and decoupling between upper crust and mantle in northeastern Tibet. *Earth Planet. Sci. Lett.*, 97, 382–403.

Tassy, A. (2007). *Recent tectonic of the Vinon-sur-Verdon thrust*. Master thesis, Université de Provence.

Tempier, C. (1987). Modèle nouveau de mise en place des structures provençales. *Bull. Soc. Géol. Fr.*, 3, 533–540.

Terrier, M. (1991). *Néotectonique de la Provence occidentale (France): vers une analyse multicritère des déformations récentes. Application à la classification des structures sismogènes*. PhD thesis, Univ. Aix-Marseille 1. Doc. BRGM 207, 232 pages.

Terrier, M., Serrano, O., and Hanot, F. (2008). Reassessment of the structural framework of western Provence (France): consequence on the regional seismotectonic model. *Geodin. Acta*, 21, 231–238.

Thomas, F. (2018). *Caractérisation des déformations récentes en Provence par une approche pluridisciplinaire: apport de la géomorphologie quantitative et de la paléosismologie*. PhD thesis, Univ. Aix-Marseille.

Thomas, F., Godard, V., Bellier, O., Benedetti, L., Ollivier, V., Rizza, M., Guillou, V., Hollender, F., Aumaître, G., Bourlès, D. L., and Keddadouche, K. (2018). Limited influence of climatic gradients on the denudation of a Mediterranean carbonate landscape. *Geomorphology*, 316, 44–58.

Thomas, F., Rizza, M., Bellier, O., Billant, J., Dussouillez, P., Fleury, J., Delanghe, D., Ollivier, V., Godard, V., and Talon, B. (2020). Assessing post-pliocene deformation in a context of slow tectonic deformation: insights from paleoseismology, remote sensing and shallow geophysics in Provence, France. *Nat. Hazards*, 105, 1453–1490.

Thouvenot, F., Frechet, J., Tapponnier, P., Thomas, J.-C., Le Brun, B., Menard, G., Lacassin, R., Jenatton, L., Grasso, J.-R., Coutant, O., Paul, A., and Hatzfled, D. (1998). The M(L) 5.3 Epagny (French Alps) earthquake of 1996 July 15: a long-awaited event on the Vuache Fault. *Geophys. J. Int.*, 135, 876–892.

Ustaszewski, K. and Schmid, S. M. (2007). Latest Pliocene to recent thick-skinned tectonics at the Upper Rhine Graben—Jura Mountains junction. *Swiss J. Geosci.*, 100, 293–312.

Van Vliet-Lanoë, B., Pissart, A., Baize, S., Brulhet, J., and Ego, F. (2019). Evidence of multiple thermokarst events in northeastern France and southern Belgium during the two last glaciations. A discussion on "Features caused by ground ice growth and decay in Late Pleistocene fluvial deposits, Paris basin, France" (Bertran et al., 2018). *Geomorphology*, 327, 613–628.

Villéger, M. (1983). Volx Moutain: a new interpretation of the tectonics. *C. R. Acad. Sci.—Ser. IIa Sci. Terre Planetes*, 297, 363–366.

Villéger, M. and Andrieux, J. (1987). Phases tectoniques post-éocènes et structuration polyphasée du panneau de couverture nord provençal (Alpes externes méridionales). *Bull. Soc. Géol. Fr.*, III(8), 147–156.

Walpersdorf, A., Sue, C., Baize, S., Cotte, N., Bascou, P., Beauval, C., Collard, P., Daniel, G., Dyer, H., Grasso, J.-R., Hautecoeur, O., Helmstetter, A., Hok, S., Langlais, M., Menard, G., Mousavi, Z., Ponton, F., Rizza, M., Rolland, L., Souami, D., Thirard, L., Vaudey, P., Voisin, C., and Martinod, J. (2015). Coherence between geodetic and seismic deformation in a context of slow tectonic activity (SW Alps, France). *J. Geodyn.*, 85, 58–65.

Wells, D. L. and Coppersmith, K. J. (1994). New empirical relationships among magnitude, rupture length, rupture width, rupture area, and surface displacement. *Bull. Seismol. Soc. Am.*, 84, 974–1002.

Wernert, P. (1957). *Stratigraphie paléontologique et préhistorique des sédiments quaternaires d'Alsace*, volume 14 of *Mémoires du Service de la carte géologique d'Alsace et de Lorraine*. Service de la carte géologique d'Alsace et de Lorraine, https://www.persee.fr/doc/sgeol_0080-9020_1957_mon_14_1.